Lecture Notes for Quantum Matter 2, TT 2024

F.H.L. Essler
The Rudolf Peierls Centre for Theoretical Physics
Oxford University, Oxford OX1 3PU, UK

April 21, 2024

Contents

Part I
Elements of Quantum Statistical Mechanics

1 Pure vs mixed states and (reduced) density matrices

Quantum states come in two categories:

1. Pure states

   These are the objects introduced in your basic Quantum Mechanics course. They are formed from complete sets of probability amplitudes and a basic assumption your lecturer will have made is that our QM system of interest was somehow prepared in such a state. In other words our basic premise was that we know the precise quantum state our system is in (at least at some initial time). Given a pure state $|\psi\rangle$ we can form an operator called the *density matrix*

   $$\rho = |\psi\rangle\langle\psi|. \tag{1}$$

   The density matrix is a convenient object for calculating expectation values, and more generally probability distributions of observables $\mathcal{O}$

   $$\langle\psi|\mathcal{O}|\psi\rangle = \text{Tr}\left[\rho \ \mathcal{O}\right] \ ,$$
   $$\langle\psi|\mathcal{O}^2|\psi\rangle - \langle\psi|\mathcal{O}|\psi\rangle^2 = \text{Tr}\left[\rho\Big(\mathcal{O} - \text{Tr}\left[\rho \ \mathcal{O}\right]\Big)^2\right], \ \text{etc.} \tag{2}$$

2. Mixed states

   More generally we need to deal with situations where our system can be in any of a set of states $\{|\psi_1\rangle, \ldots, |\psi_N\rangle\}$ and the best we can do is to know the associated probabilities $\{p_1, \ldots, p_N\}$. This results in a density matrix of the form

   $$\rho_{\text{mixed}} = \sum_{j=1}^{N} p_j |\psi_j\rangle\langle\psi_j|. \tag{3}$$

   Note that in general this cannot be written in the form (1). An example you actually have encountered before is the Stern-Gerlach experiment. Here the oven creates silver atoms with random spin orientations, i.e. 50-50 mixtures of $|\uparrow\rangle$ and $|\downarrow\rangle$. The resulting density matrix described a mixed state

   $$\rho = \frac{1}{2}|\uparrow\rangle\langle\uparrow| + \frac{1}{2}|\downarrow\rangle\langle\downarrow| = \frac{1}{2}\mathbb{1}. \tag{4}$$

   In this state we have

   $$\text{Tr}\left[\rho S^\alpha\right] = 0 \ , \tag{5}$$

   so the beam is indeed unpolarized. In contrast the pure state

   $$|\psi\rangle = \frac{1}{\sqrt{2}}\left[|\downarrow\rangle - |\uparrow\rangle\right] \ , \quad \rho_\psi = |\psi\rangle\langle\psi| \tag{6}$$

   describes a beam polarized in the x-direction

   $$\text{Tr}\left[\rho_\psi S^\alpha\right] = \delta_{\alpha,x} \ . \tag{7}$$

It is clear from their definition that density matrices have real, positive eigenvalues that sum up to one.

1.1 Relation between pure and mixed states

Consider a composite system, but measure only part A of it. This gives us access to

$$\text{Tr}\left[\rho\mathcal{O}_A\right] \ , \tag{8}$$

where $\mathcal{O}_A$ acts non-trivially only on the subsystem A (and as the identity operator on its complement $\bar{A}$). A basis of states of the entire system can be obtained from the states

$$|e_{A,j}\rangle \otimes |e_{\bar{A},k}\rangle \ , \quad j = 1, \ldots, \dim(\mathcal{H}_A) \ , \quad k = 1, \ldots, \dim(\mathcal{H}_{\bar{A}}) \tag{9}$$

where $\{|e_{A,j}\rangle\}$ and $\{|e_{\bar{A},k}\rangle\}$ form orthnormal bases of the Hilbert spaces $\mathcal{H}_A$ and $\mathcal{H}_{\bar{A}}$ associated with subsystem A and $\bar{A}$ respectively. We therefore have

$$\text{Tr}\left[\rho\mathcal{O}_A\right] = \text{Tr}_A\left[\rho_A\mathcal{O}_A\right] , \quad \rho_A = \text{Tr}_{\bar{A}}\left[\rho\right]. \tag{10}$$

The operator ρ_A is called *reduced density matrix* (RDM) of subsystem A. Here comes the point: *the RDM of a pure state is generally mixed.* As an example consider a 2-qbit system in the pure state

$$|\psi\rangle = \alpha|\uparrow\downarrow\rangle + \beta|\downarrow\uparrow\rangle , \qquad |\alpha|^2 + |\beta|^2 = 1. \tag{11}$$

We have

$$\rho_\psi = |\alpha|^2|\uparrow\downarrow\rangle\langle\uparrow\downarrow| + |\beta|^2|\downarrow\uparrow\rangle\langle\downarrow\uparrow| + \alpha\beta^*|\uparrow\downarrow\rangle\langle\downarrow\uparrow| + \alpha^*\beta|\downarrow\uparrow\rangle\langle\uparrow\downarrow| ,$$
$$\text{Tr}_2\big(\rho_\psi\big) = |\alpha|^2|\uparrow\rangle\langle\uparrow| + |\beta|^2|\downarrow\rangle\langle\downarrow|. \tag{12}$$

This is a mixed state because we don't have any knowledge about qbit 2.

1.2 (R)DM for spin-1/2 models

Consider a composite system of L spin-1/2s (or equivalently qbits). Each of the spins lives on a site of a lattice. A basis of states is provided by the product states

$$|\sigma_1\rangle \otimes |\sigma_2\rangle \otimes \cdots \otimes |\sigma_L\rangle , \quad \sigma_j \in \{\uparrow, \downarrow\}. \tag{13}$$

A basis of operators acting on the spin on site j is then given by

$$\sigma_j^\alpha , \quad \alpha = 0, 1, 2, 3 , \quad \sigma_j^0 = \mathbb{1}_j , \tag{14}$$

where $\sigma_j^{1,2,3}$ are the Pauli matrices. Expressing the density matrix in this basis gives

$$\rho = \sum_{\alpha_1,\ldots,\alpha_L} \rho_{\alpha_1,\ldots,\alpha_L} \ \sigma_1^{\alpha_1}\ldots\sigma_L^{\alpha_L}. \tag{15}$$

Hence

$$\text{Tr}\left[\rho\sigma_1^{\beta_1}\ldots\sigma_L^{\beta_L}\right] = \sum_{\alpha_1,\ldots,\alpha_L} \rho_{\alpha_1,\ldots,\alpha_L} \underbrace{\text{Tr}\left[\sigma_1^{\alpha_1}\ldots\sigma_L^{\alpha_L}\sigma_1^{\beta_1}\ldots\sigma_L^{\beta_L}\right]}_{\prod_{j=1}^L \text{Sp}_{2\times 2}[\sigma_j^{\alpha_j}\sigma_j^{\beta_j}]=\prod_{j=1}^L 2\delta_{\alpha_j,\beta_j}} = 2^L \rho_{\beta_1\ldots\beta_L}. \tag{16}$$

This shows that the expansion coefficients $\rho_{\alpha_1,\ldots,\alpha_L}$ are nothing but the equal time spin correlation functions in the state ρ.

For RDMs excatly the same analysis applies with the sites restricted to the subsystem, so that

$$\rho_A = \frac{1}{2^\ell} \sum_{\alpha_1,\ldots,\alpha_\ell} \text{Tr}\left[\rho \ \sigma_{j_1}^{\alpha_1}\ldots\sigma_{j_\ell}^{\alpha_\ell}\right]\sigma_{j_1}^{\alpha_1}\ldots\sigma_{j_\ell}^{\alpha_\ell}. \tag{17}$$

2 Entropy and equilibrium ensembles

Given a density matrix we can define the associated von Neumann entropy

$$S = -\text{Tr}\big[\rho\ln\rho\big]. \tag{18}$$

In the orthonormal eigenbasis of the density matrix we have

$$\rho = \sum_\alpha p_\alpha|\alpha\rangle\langle\alpha| , \tag{19}$$

4

and hence

$$S = -\sum_\alpha p_\alpha \ln p_\alpha .$$

(20)

Given a Hamiltonian H with $H|n\rangle = E_n|n\rangle$ the equilibrium ensembles of Statistical Mechanics are defined through the following density matrices:

- Gibbs ensemble

$$\rho_G = \frac{1}{Z} e^{-\beta H} , \quad \beta = \frac{1}{k_B T} , \qquad Z = \text{Tr}[e^{-\beta H}].$$

(21)

- Microcanonical ensemble

$$\rho_{\text{MC}} = \frac{1}{\mathcal{N}_\delta} \sum_{|E_n - E(\beta)| < \delta} |n\rangle \langle n|$$

(22)

Here the energy density $E(\beta)$ corresponding to inverse temperature β is determined by

$$\frac{\partial S}{\partial E} = \beta.$$

(23)

These density matrices become *locally equivalent* in the thermodynamic limit:

$$\lim_{L\to\infty} \text{Tr}\left[\rho_G \mathcal{O}_A\right] = \lim_{L\to\infty} \text{Tr}\left[\rho_{\text{MC}} \mathcal{O}A\right] \ \forall \text{ local operators } \mathcal{O}_A.$$

(24)

Here a local operator is characterized by the property that it acts non-trivially only in a finite, local region in space.

2.1   RDM of the Gibbs ensemble

Let us consider the RDM of a Gibbs density matrix

$$\rho_{G,A} = \text{Tr}_{\bar{A}}\left[\frac{1}{Z} e^{-\beta H}\right] .$$

(25)

We can write this in the form

$$\rho_{G,A} = \frac{1}{Z^{(A)}} e^{-\beta H^{(A)}} .$$

(26)

However, the operator $H^{(A)}$ is not simply the restriction of the full Hamiltonian H to the subsystem A

$$H^{(A)} \neq H\Big|_A.$$

(27)

To see how the two differ let's consider a Gibbs ensemble of a lattice model at a high temperature, where we have a finite correlation length

$$\text{Tr}\left[\rho_G \ \mathcal{O}_j^\dagger \mathcal{O}_k\right] \propto e^{-\frac{d(j,k)}{\xi_\mathcal{O}}} .$$

(28)

Here $\mathcal{O}_j$ is a local operator acting in the vicinity of site j and $d(j,k)$ is the spatial separation between the regions in which the two operators acts non-trivially.

2.1.1 High-temperature expansion

At high temperature we can expand everything in powers of β

$$\rho_{\mathrm{G}} = \frac{1}{Z}\left[\mathbb{1} - \beta H - \frac{\beta^2}{2}H^2 - \dots\right] , \qquad Z = \underbrace{\mathrm{Tr}(\mathbb{1})}_{D} - \beta\langle H\rangle + \frac{\beta^2}{2}\langle H^2\rangle + \dots ,$$

$$Z^{-1} = \frac{1}{D}\left[1 + \frac{\beta}{D}\langle H\rangle + \dots\right] , \qquad \langle \mathcal{O}\rangle \equiv \mathrm{Tr}[\mathcal{O}]. \tag{29}$$

This gives a high-temperature expansion of the DM in the form

$$\rho_{\mathrm{G}} = \frac{1}{D}\left[\mathbb{1} - \beta\left(H - \frac{\langle H\rangle}{D}\right) + \frac{\beta^2}{2}\left(H - \frac{\langle H\rangle}{D}\right)^2 + \dots\right]. \tag{30}$$

In order to work out what $H^{(A)}$ looks like we decompose the Hamiltonian as

$$H = H_A + H_{\bar{A}} + H_{A\bar{A}} , \tag{31}$$

where H_A ($H_{\bar{A}}$)acts only on subsystem A ($\bar{A}$) and $H_{A\bar{A}}$ is localized at the boundary of A (we assume short-ranged interactions).
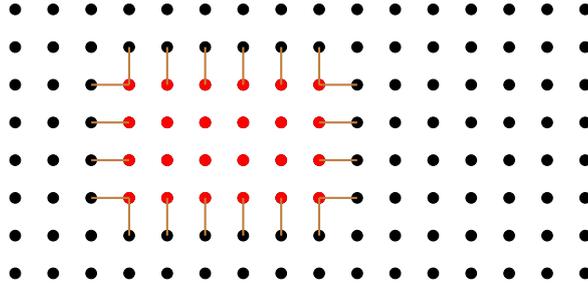
Figure 1: Red sites: sub-system A. Brown lines: interactions described by the Hamiltonian $H_{A\bar{A}}$.

$$\rho_{\mathrm{G},A} = \frac{1}{D_A}\left[\mathbb{1}_A - \beta\left(H_A - \frac{\langle H_A\rangle_A}{D_A}\right) - \beta\left(\frac{\langle H_{A\bar{A}}\rangle_{\bar{A}}}{D_{\bar{A}}} - \frac{\langle H_{A\bar{A}}\rangle}{D}\right) + \dots\right] \tag{32}$$

Here $\langle H_{A\bar{A}}\rangle_{\bar{A}} - \mathrm{Tr}_{\bar{A}}(H_{A\bar{A}})$ is an operator that acts non-trivially only close to the boundary of A. We conclude that at leading order in β

$$H^{(A)} = H_A + \text{ boundary contribution }. \tag{33}$$

> **Exercise 1: $\mathcal{O}(\beta^2)$ contribution**
>
> Work out the form of the second order in β contribution to $\rho_{\mathrm{G},A}$ and show that it again is localized in the vicinity of the boundary.

2.2 MC ensemble and typicality

We need to make one more comment on the MC ensemble, which we recall is defined in terms of energy eigenstates $|n\rangle$ with energies E_n as

$$\rho_{\mathrm{MC}} = \frac{1}{\mathcal{N}_\delta} \sum_{|E_n - E(\beta)| < \delta} |n\rangle\langle n| . \tag{34}$$

If we randomly pick any of the terms in the sum over the MC shell, say $|m\rangle$, then with a probability exponentially close (in system size) to 1 ($|p - 1| \propto e^{-\alpha L}$) the expectation value in state $|m\rangle$ is the same as the MC average up to finite-size corrections that vanish in the thermodynamic limit

$$\mathrm{Tr}\big[\rho_{\mathrm{MC}}\mathcal{O}_A\big] = \langle m|\mathcal{O}_A|m\rangle + o(L). \tag{35}$$

This implies two things:

- Almost all energy eigenstates in a finite energy shell at any finite energy density are *locally thermal*, i.e. their local properties are the same (up to finite-size corrections) and given by the thermal averages.

- We can definite the MC ensemble in terms of a single *typical* eigenstate.

Part II
EIGENSTATES OF LOCAL MANY-PARTICLE HAMILTONIANS

We now take a closer look at energy eigenstates of many-particle Hamiltonians with local densities. In particular we want to get a qualitative understanding of their entanglement properties.

3 Tight-binding model of spinless fermions

In general it is very difficult to determine exact eigenstates of many-particle Hamiltonians. An exception to this rule that you have encountered before are non-interacting models. We start by considering one such example: the tight-binding model of spinless fermions in one spatial dimension

$$H = -J\sum_{j=1}^{L} c_j^\dagger c_{j+1} + c_{j+1}^\dagger c_j - \mu \sum_j c_j^\dagger c_j . \tag{36}$$

This can be diagonalizd by going to momentum space

$$c(k) = \frac{1}{\sqrt{L}} \sum_j e^{ikj} c_j , \quad k \in \{\frac{2\pi n}{L}|n = -\frac{L}{2}+1, \ldots, \frac{L}{2}\}. \tag{37}$$

We find

$$H = \sum_k \underbrace{\big(-2J\cos(k) - \mu\big)}_{\epsilon(k)} c^\dagger(k)c(k) . \tag{38}$$

Assuming that the chemical potential is such that $|\mu/2J| < 1$ the ground state is obtained as a Fermi sea

$$|\mathrm{GS}\rangle = \prod_{|k|<k_F} c^\dagger(k)|0\rangle , \quad k_F = \arccos\big(\frac{\mu}{2J}\big) . \tag{39}$$

Here $|0\rangle$ is the fermion vacuum defined by $c(k)|0\rangle = 0$ and the ground state energy is

$$E_{\mathrm{GS}} = \sum_{|k|<k_F} \epsilon(k) . \tag{40}$$

As we are dealing with a lattice model there is a state of maximal energy, which is simply the ground state of $-H$. Low-lying excitations are obtained by making particle and hole excitations in the vicinity of the Fermi points $\pm k_F$. For example, if we make a single-particle hole excitation we obtain an excitation energy

$$E(k_p, k_h) - E_{\mathrm{GS}} = \epsilon(k_p) - \epsilon(k_h) , \quad |k_h| < k_F < |k_p|. \tag{41}$$

7

If $k_{p,h} \approx \pm k_F$ we can linearize the dispersion relation arpound k_F and e.g. for $k_{p,h} \approx k_F$ obtain

$$E(k_p, k_h) - E_{\mathrm{GS}} \approx v_F(k_p - k_h) , \qquad v_F = \epsilon'(k_F). \tag{42}$$

This tells us that our spectrum is gapless in the thermodynamic limit, and in a finite system the excitation gap scales as L^{-1} (due to the quantization condition for the single-particle momenta). This in turns tells us that the level spacing between excited states scales linearly in L^{-1}. This means that if we take a finite energy window above the ground state energy, there will only be a polynomial number (in L) of energy eigenstates inside the window.

Let us now consider energy eigenstates at a finite energy density e above the ground state, i.e. states with eigenvaluyes E such that the extensive part of the excitation energy is eL

$$(E - E_{\mathrm{GS}}) = Le + o(L) . \tag{43}$$

We know from Statistical Mechanics that the maximal extropy "state" at a finite energy density corresponds to the Fermi-Dirac distribution

$$n(k) = \frac{1}{1 + e^{\epsilon(k)/T}} , \tag{44}$$

where the temperature T is related to the energy density e by

$$e = \int_{-\pi}^{\pi} \frac{dk}{2\pi} \, n(k) \, \epsilon(k) . \tag{45}$$

We can then construct thermal micro-states by considering momentum space Fock states (which are automatically energy eigenstates in our tight-binding model)

$$|\boldsymbol{k}\rangle = \prod_{j=1}^{N} c^{\dagger}(k_j)|0\rangle, \tag{46}$$

such that the k_j are distributed according to the Fermi-Dirac distribution function $n(k)$

$$n(k)\Delta k = \frac{2\pi}{L} \times \text{ number of } k_j \text{ in } [k, k + \Delta k] . \tag{47}$$

Thermodynamics tells us that there are exponentially many such states in a finite energy window, because their number is by definition proportional to the exponential of the entropy e^S, and S itself is extensive $S \propto L$. This is turn tells us that the spacing between adjacent energy levels is exponentially small. Combining our various observations we conclude that the many-particle energy level spacing has the structure shown in Fig. 3.

4 Entanglement and entanglement measures

Entanglement refers to the property of most quantum states of composite systems (a simple example for a 2-qbit system is $|\uparrow\downarrow\rangle + |\downarrow\uparrow\rangle$) that measuring one part affects subsequent measurements of the other part. The exceptions are *product states*, e.g. $|\uparrow\downarrow\rangle$, which have no entanglement. A natural question to ask is whether we can *quantify* entanglement. To quote a prominent recent Nobel Prize winner: "Yes, we can!".

4.1 Bipartite entanglement entropy for pure states

Let $|\Psi\rangle$ be a pure state and denote the associated reduced density matrix of sub-system A by

$$\rho_A = \mathrm{Tr}_{\bar{A}}\Big[|\Psi\rangle\langle\Psi|\Big]. \tag{48}$$

The *bipartite entanglement entropy* of subsystem A is then defined as the von Neumann entropy of the subsystem

$$S_A = -\mathrm{Tr}\Big[\rho_A \ln(\rho_A)\Big] = -\mathrm{Tr}\Big[\rho_{\bar{A}} \ln(\rho_{\bar{A}})\Big]. \tag{49}$$

The second identity can be established by using the following two theorems from Linear Algebra.
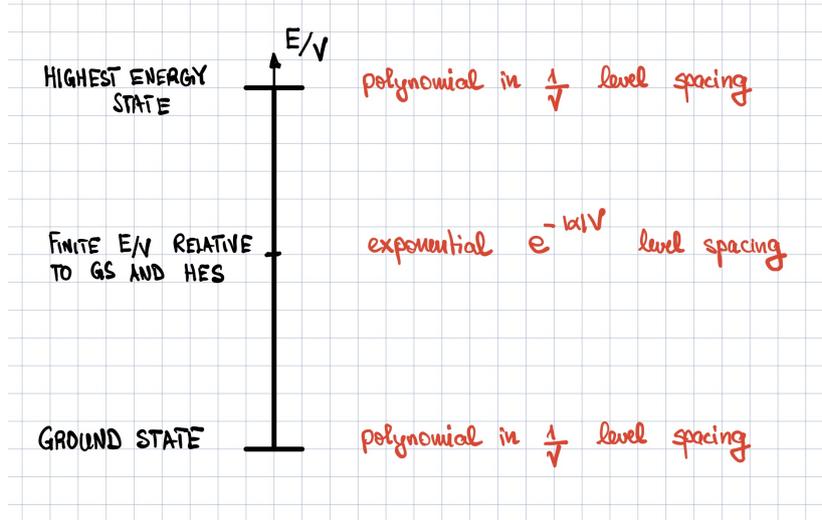
Figure 2: Structure of the energy level spacing in many-particle lattice models with translationally invariant Hamiltonians with local densities.

Theorem 1 *Singular Value Decomposition*

Let M be an $m \times n$ complex valued matrix. Then there exist (non-unique) $m \times m$ unitary matrices U, $n \times n$ unitary matrices V and diagonal, real positive matrices Σ such that

$$\boxed{M = U\Sigma V^{\dagger}}$$

(50)

Theorem 2 *Schmidt Decomposition Let $\mathcal{H} = \mathcal{H}_A \otimes \mathcal{H}_B$ be a linear vector space, and $|\psi\rangle \in \mathcal{H}$. Then there exists orthonormal bases $\{|w_1^A\rangle, \ldots, |w_n^A\rangle,\}$ of $\mathcal{H}_A$ and $\{|w_1^B\rangle, \ldots, |w_m^B\rangle,\}$ of $\mathcal{H}_B$ such that*

$$\boxed{|\psi\rangle = \sum_{\alpha=1}^{\min(m,n)} \lambda_\alpha |w_\alpha^A\rangle \otimes |w_\alpha^B\rangle}$$

(51)

The Schmidt coefficients fulfil $\lambda_\alpha \geq 0$ and $\sum_\alpha |\lambda_\alpha|^2 = 1$.

Aside 1

The Schmidt decomposition immediately follows from the SVD as we will now demonstrate. Let us start by expanding $|\psi\rangle$ in the tensor product basis of $\mathcal{H}$ and assume without loss of generality that $n \geq m$

$$|\psi\rangle = \sum_{i=1}^{n}\sum_{j=1}^{m} \psi_{ij} |e_i^A\rangle \otimes |e_j^B\rangle .$$

(52)

Viewing ψ_{ij} as a complex $n \times m$ matrix we can apply the SVD to obtain

$$\psi = U \begin{pmatrix} \Sigma \\ 0_{m\times(n-m)} \end{pmatrix} V^{\dagger},$$

(53)

where Σ is a diagonal $m \times m$ matrix. In components this reads

$$\psi_{ij} = \sum_{k,\ell=1}^{m} U_{i,k} \lambda_k \delta_{k,\ell} V_{\ell,j}^{\dagger} .$$

(54)

9

Defining

$$|w_k^A\rangle = \sum_{i=1}^{n} U_{i,k}|e_i^A\rangle \ , \qquad |w_\ell^B\rangle = \sum_{j=1}^{m} V_{\ell,j}^\dagger|e_j^B\rangle \ , \tag{55}$$

and substituting back in (52) we arrive at the Schmidt decomposition.

Let us now apply the Schmidt decomposition to the bipartite entanglement entropy. We have

$$\rho = |\psi\rangle\langle\psi| \ , \qquad |\psi\rangle = \sum_{\alpha=1}^{\min(m,n)} \lambda_\alpha |w_\alpha^A\rangle \otimes |w_\alpha^B\rangle \ , \tag{56}$$

which gives

$$\rho = \sum_{\alpha,\beta} \lambda_\alpha \lambda_\beta \Big(|w_\alpha^A\rangle \otimes |w_\alpha^B\rangle\Big)\Big(\langle w_\beta^A| \otimes \langle w_\beta^B|\Big). \tag{57}$$

The RDM of subsystem A is then simply

$$\rho_A = \sum_\gamma \langle w_\gamma^B|\rho|w_\gamma^b\rangle = \sum_\alpha \lambda_\alpha^2 |w_\alpha^A\rangle\langle w_\alpha^A|. \tag{58}$$

Similarly we obtain

$$\rho_B = \sum_\alpha \lambda_\alpha^2 |w_\alpha^B\rangle\langle w_\alpha^B|. \tag{59}$$

Hence we have

$$\boxed{S_A = \sum_{\alpha=1}^{\min(m,n)} \lambda_\alpha^2 \ln \lambda_\alpha^2 = S_B \ .}$$

$$\tag{60}$$

4.2 Bipartite entanglement entropy of energy eigenstates

The bipartite entanglement entropy (BEE) of energy eigenstates in many-particle systems with local Hamiltonians has the structure shown in Fig. 4.2 States in the vicinity of the "edges" of the spectrum have low
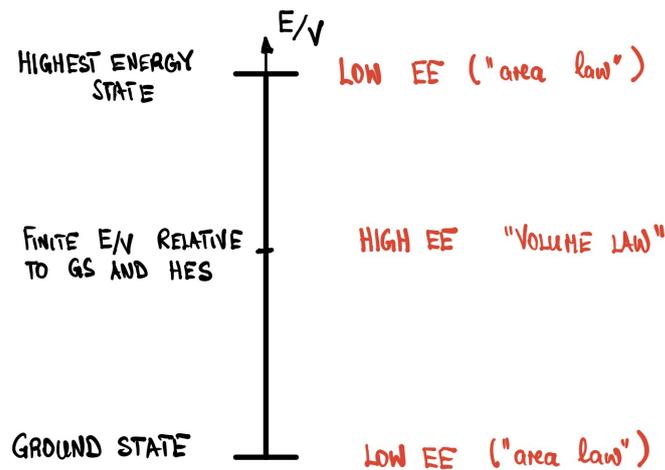
Figure 3: Structure of EE of energy eigenstates in many-particle lattice models with translationally invariant Hamiltonians with local densities.

entanglement and follow an "area law". By "vicinity of the ground state" we mean states with energies such that for large V

$$E - E_{\text{GS}} \propto V^0 , \qquad (61)$$

and "area law" means that, to logarithmic (in the volume of A) accuracy, the EE is proportional to the size of the boundary of the subsystem A

$$S_A \propto |\partial A|. \qquad (62)$$

We will see an example of this is the next section. Eigenstates with energies that differ from E_{GS} and E_{HES} by extensive amounts "typically" obey a volume law. This means that if we randomly pick an energy eigenstate at the energy density of interest, its BEE will be proportional to the size of the subsystem with a probability that is exponentially close (in the size of the entire system) to 1

$$S_A \propto |A| \qquad \text{with probability } 1 + \mathcal{O}(e^{-\text{const}V}). \qquad (63)$$

The volume law for such states can be readily understood by means of the following argument. The density matrix we are interested in is in fact just the micro-canonical ensemble formed with a single eigenstate

$$\rho_{\text{MC}} = |E\rangle\langle E| . \qquad (64)$$

As we have argued above, the RDM for a finite subsystem is (up to finite size corrections that go to zero as we increase the total volume V) the same as the one obtained from the Gibbs ensemble

$$\rho_{\text{MC},A} = \rho_{\text{G},A} . \qquad (65)$$

As long as we stay away from energy densities that correspond to temperatures at which phase transitions occur, the state $|E\rangle$ will have a finite correlation length ξ_E. This is turn allows us to approximate

$$\rho_{\text{G},A} \approx \frac{1}{\tilde{Z}_A} e^{-\beta \tilde{H}_A} , \qquad (66)$$

where $\tilde{H}_A$ is well approximated by the restriction of H to the subsystem, except in a vicinity of order ξ_E of its boundary. In any case, it has good locality properties. The BEE is then simply the thermodynamic entropy of a system with Hamiltonian $\tilde{H}_A$, which we know to be extensive

$$S_A \propto |A|. \qquad (67)$$

5 The spin-1 AKLT (Affleck-Kennedy-Lieb-Tasaki) chain

Ground states of many-particle systems are generally very difficult to determine exactly. We now discuss a famous example where this is possible. This will lead us to introduce *matrix-product states* (MPS), which provide the basis for the best available numerical methods for computing ground state properties of low-dimensional systems. En passant we get to understand *symmetry-protected topological order* and the *Haldane conjecture*. The Hamiltonian of the spin-1 AKLT chain is

$$H = \sum_{j=1}^{L} \frac{1}{2} \boldsymbol{S}_j \cdot \boldsymbol{S}_{j+1} + \frac{1}{6} \big(\boldsymbol{S}_j \cdot \boldsymbol{S}_{j+1} \big)^2 + \frac{1}{3}. \qquad (68)$$

Here S_j^α are spin-1 operators on site j of a ring and $S_{L+1}^\alpha \equiv S_1^\alpha$. On each site we have 3 linearly independent states, which we can take to be the eigenstates of S_j^z (with eigenvalues 1, 0 and -1 respectively)

$$|+\rangle_j , \qquad |0\rangle_j , \qquad |-\rangle_j . \qquad (69)$$

In the following we will need to know the eigenstates of the angular momentum operators for a pair of sites. You know these from the "addition of angular momentum" part of your Quantum Mechanics course. The maximal set of commtuing spin operators for a two-site system is

$$\boldsymbol{S}_1^2 \ , \quad \boldsymbol{S}_2^2 \ , \quad S^z \equiv S_1^z + S_2^z \ , \quad \boldsymbol{S}^2 \equiv (\boldsymbol{S}_1 + \boldsymbol{S}_2)^2. \tag{70}$$

The simultaneous eigenstates of these operators are $|S, s_z, S_1, S_2\rangle$, where

$$\boldsymbol{S}^2|S, s_z, S_1, S_2\rangle = S(S+1)|S, s_z, S_1, S_2\rangle \ ,$$
$$S^z|S, s_z, S_1, S_2\rangle = s_z|S, s_z, S_1, S_2\rangle \ ,$$
$$\boldsymbol{S}_a^2|S, s_z, S_1, S_2\rangle = S_a(S_a+1)|S, s_z, S_1, S_2\rangle \ , \ a = 1, 2. \tag{71}$$

They form three SU(2) representations: a quintet, a triplet and a singlet

$$\text{S=2 quintet: } |2, 2, 1, 1\rangle = |++\rangle = |+\rangle_1 \otimes |+\rangle_2 \ ,$$
$$|2, 1, 1, 1\rangle = \frac{1}{\sqrt{2}}(|+0\rangle + |0+\rangle) \ ,$$
$$|2, 0, 1, 1\rangle = \frac{1}{\sqrt{6}}(|+-\rangle + |-+\rangle + 2|00\rangle) \ ,$$
$$|2, -1, 1, 1\rangle = \frac{1}{\sqrt{2}}(|-0\rangle + |0-\rangle) \ ,$$
$$|2, -2, 1, 1\rangle = |--\rangle \ ,$$
$$\text{S=1 triplet: } |1, 1, 1, 1\rangle = \frac{1}{\sqrt{2}}(|+0\rangle - |0+\rangle) \ ,$$
$$|1, 0, 1, 1\rangle = \frac{1}{\sqrt{2}}(|+-\rangle - |-+\rangle) \ ,$$
$$|1, -1, 1, 1\rangle = \frac{1}{\sqrt{2}}(|-0\rangle - |0-\rangle) \ ,$$
$$\text{S=0 singlet: } |0, 0, 1, 1\rangle = \frac{1}{\sqrt{3}}(|+-\rangle + |-+\rangle - |00\rangle) \ . \tag{72}$$

We now write the Hamiltomnian in a form where its action on these states will take a very simple form. To that end observe that

$$\boldsymbol{S}_1 \cdot \boldsymbol{S}_2 = \frac{1}{2}\left[\boldsymbol{S}^2 - \boldsymbol{S}_1^2 - \boldsymbol{S}_1^2\right] = \frac{1}{2}\left[2 \ 3P_{12}^{(S=2)} + 1 \ 2P_{12}^{(S=1)} - 0 \ 1 \ P_{12}^{(S=0)} - 2 - 2\right], \tag{73}$$

where $P_{12}^{(S)}$ are projection operators on the spin-S representations above. Taking the square of (73) gives for the biquadratic term

$$(\boldsymbol{S}_1 \cdot \boldsymbol{S}_2)^2 = -3P_{12}^{(S=2)} - 3P_{12}^{(S=1)} + 4 \ , \tag{74}$$

and hence the Hamiltonian becomes a sum over projection operators onto the spin-2 representation for each pair of neighbouring sites

$$H = \sum_{j=1}^{L} P_{j,j+1}^{(S=2)} \ . \tag{75}$$

As the projection operators have eigenvalues 1 and 0 a lower bound for the ground state energy of (75) is $E = 0$. Hence, if we can find a state such that

$$P_{j,j+1}^{(S=2)}|\psi\rangle = 0 \ \forall j \tag{76}$$

then this state will necessarily be a ground state. Hamiltonians that can be written as sums over local operators H_j that have ground states that are simultaneous eigenstates of of all H_j are called *frustration free*.

5.1 Ground state of the AKLT chain

We will now prove that the ground state of the AKLT chain can be written as a *matrix-product state*

$$|\text{GS}\rangle = \sum_{\sigma_1,\ldots,\sigma_L} \underbrace{A^{\sigma_1}_{\alpha_1\alpha_2} A^{\sigma_2}_{\alpha_2\alpha_3} \ldots A^{\sigma_L}_{\alpha_L\alpha_1}}_{\text{Tr}(A^{\sigma}_1\ldots A^{\sigma}_L)} |\sigma_1,\sigma_2,\ldots,\sigma_L\rangle . \tag{77}$$

Here A^σ are 2×2 matrices

$$A^+ = -\frac{1}{\sqrt{2}}\begin{pmatrix} 0 & 0 \\ 1 & 0 \end{pmatrix} , \qquad A^0 = \frac{1}{2}\begin{pmatrix} 1 & 0 \\ 0 & -1 \end{pmatrix} , \qquad A^- = -\frac{1}{\sqrt{2}}\begin{pmatrix} 0 & 1 \\ 0 & 0 \end{pmatrix} . \tag{78}$$

There is a very useful graphical representation for matrix product states, which is shown in Fig. 5.1.
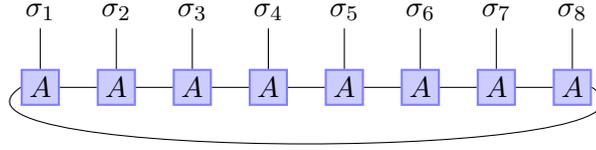
Figure 4: Graphical representation of $\text{Tr}(A^{\sigma_1}\ldots A^{\sigma_8})$.

Carrying out the sums over σ_j in (77) gives rise to 2×2 matrices of quantum states

$$|\text{GS}\rangle = \text{Tr}(g_1 \otimes g_2 \cdots \otimes g_L) ,$$
$$g_j \equiv A^{\sigma_j}|\sigma_j\rangle_j = \begin{pmatrix} \frac{1}{2}|0\rangle_j & \frac{1}{\sqrt{2}}|-\rangle_j \\ -\frac{1}{\sqrt{2}}|+\rangle_j & -\frac{1}{2}|0\rangle_j \end{pmatrix} , \tag{79}$$

and

$$H|\text{GS}\rangle = \sum_{j=1}^{L} \text{Tr}\left(g_1 \otimes g_2 \cdots \otimes g_{j-1} \otimes \left[P^{(S=2)}_{j,j+1}\left(g_j \otimes g_{j+1}\right)\right] \otimes g_{j+2} \otimes \cdots \otimes g_L\right) . \tag{80}$$

using the explicit form of the matrices g_j we find

$$g_j \otimes g_{j+1} = \begin{pmatrix} \frac{1}{4}|0\rangle_j|0\rangle_{j+1} - \frac{1}{2}|-\rangle_j|+\rangle_{j+1} & \frac{1}{\sqrt{8}}\left(|0\rangle_j|-\rangle_{j+1} - |-\rangle_j|0\rangle_{j+1}\right) \\ \frac{1}{\sqrt{8}}\left(|0\rangle_j|+\rangle_{j+1} - |+\rangle_j|0\rangle_{j+1}\right) & \frac{1}{4}|0\rangle_j|0\rangle_{j+1} - \frac{1}{2}|+\rangle_j|-\rangle_{j+1} \end{pmatrix} . \tag{81}$$

Importantly all states occcurring in (81) are linear combinations of the triplet and singlet states in (72) and do not imvolve the quintet states. Hence

$$P^{(S=2)}_{j,j+1}\left(g_j \otimes g_{j+1}\right) = \begin{pmatrix} 0 & 0 \\ 0 & 0 \end{pmatrix} , \tag{82}$$

and concomitantly $H|\text{GS}\rangle = 0$. This proves that $|\text{GS}\rangle$ is indeed a ground state of the model. It can be shown that the ground state is unique, and that there is a finite gap to excited states (known as *Haldane gap*). The state we have calculated is not normalized. We now determine its normalization. In our graphical notations $\langle\text{GS}|\text{GS}\rangle$ is represented by the diagram shown in Fig. 5.1. We observe that this can be written as a contraction of building blocks of the form shown in Fig. 5.1. As α, β take two values each $\tilde{A}$ can be viewed as a 4×4 matrix. Choosing the identification $(\alpha, \beta) \to a$ with

$$(1,1) \to 1 , \ (2,2) \to 2 , \ (1,2) \to 3 , \ (2,1) \to 4 \tag{83}$$
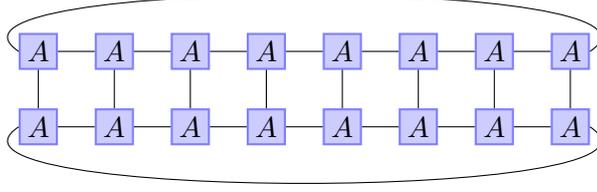
Figure 5: Graphical representation of $\langle \mathrm{GS}|\mathrm{GS}\rangle$.
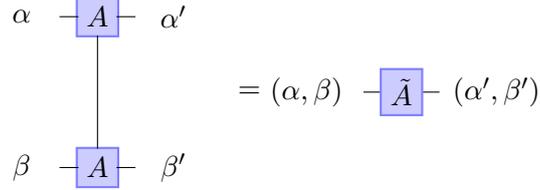
Figure 6: Building block $\tilde{A}$.

we can easily work out $\tilde{A}_{ab}$ using the explicit forms of A^σ

$$
\tilde{A} = \begin{pmatrix} \frac{1}{4} & \frac{1}{2} & 0 & 0 \\ \frac{1}{2} & \frac{1}{4} & 0 & 0 \\ 0 & 0 & -\frac{1}{4} & 0 \\ 0 & 0 & 0 & -\frac{1}{4} \end{pmatrix}.
$$
(84)

This allows us to write the normed squared of $|\mathrm{GS}\rangle$ as

$$
\langle \mathrm{GS}|\mathrm{GS}\rangle = \mathrm{Tr}_{4\times4}\left[\tilde{A}\ldots\tilde{A}\right].
$$
(85)

The eigenvalues of $\tilde{A}$ are $3/4$, $-1/4$, $-1/4$ and $-1/4$, which immediately gives us

$$
\langle \mathrm{GS}|\mathrm{GS}\rangle = \left(\frac{3}{4}\right)^L + 3\left(-\frac{1}{4}\right)^L.
$$
(86)

Nice.

5.2 Spin-spin correlation functions

We now turn to spin-spin correlatiuon functions. Introducing short-hand notations such that $|\boldsymbol{\sigma}\rangle = |\sigma_1,\ldots,\sigma_L\rangle$ we can write these (modulo the normalization of $|\mathrm{GS}\rangle$) as

$$
\langle \mathrm{GS}|S_1^z S_{r+1}^z|\mathrm{GS}\rangle = \sum_{\boldsymbol{\sigma},\boldsymbol{\sigma'}}\langle\boldsymbol{\sigma}|\mathrm{Tr}[A^{\sigma_1}\ldots A^{\sigma_L}]\sigma_1\sigma_{r+1}\mathrm{Tr}[A^{\sigma'_1}\ldots A^{\sigma'_L}]|\boldsymbol{\sigma'}\rangle.
$$
(87)

Here we have used that $\langle\sigma_j|S_j^z = \sigma_j\langle\sigma_j|$. In our graphical notations this can be written in the form shown in Fig. 5.2.

We can again use the transfer matrix formalism we employed for computing the normalization for the ground state. To do so we need to introduce one new building block, *cf.* Fig. 5.2. The corresponding 4×4 matrix can be worked out in the same way as $\tilde{A}$

$$
\tilde{B} = \begin{pmatrix} 0 & -\frac{1}{2} & 0 & 0 \\ \frac{1}{2} & 0 & 0 & 0 \\ 0 & 0 & 0 & 0 \\ 0 & 0 & 0 & 0 \end{pmatrix}.
$$
(88)
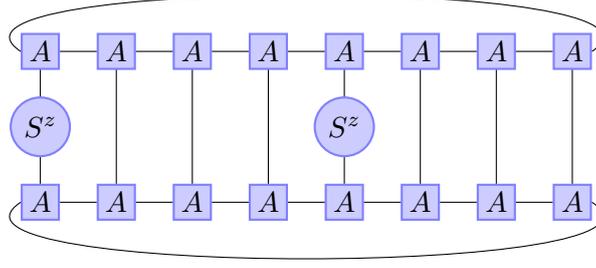
Figure 7: Graphical representation of the (unnormalized) spin-spin correlator for $L = 8$, $r = 4$.

Figure 8: Building block $\tilde{B}$.

In terms of our matrices $\tilde{A}$ and $\tilde{B}$ we then have

$$\langle \mathrm{GS}|S_1^z S_{r+1}^z|\mathrm{GS}\rangle = \mathrm{Tr}_{4\times 4}\Big[\tilde{B}\tilde{A}^{r-1}\tilde{B}\tilde{A}^{L-r-1}\Big]. \tag{89}$$

Due to the structure of $\tilde{B}$ this reduces to the trace of the upper left 2×2 block only

$$\langle \mathrm{GS}|S_1^z S_{r+1}^z|\mathrm{GS}\rangle = \mathrm{Tr}_{2\times 2}\Big[\begin{pmatrix} 0 & -\frac{1}{2} \\ \frac{1}{2} & 0 \end{pmatrix}\begin{pmatrix} \frac{1}{4} & \frac{1}{2} \\ \frac{1}{2} & \frac{1}{4} \end{pmatrix}^{r-1}\begin{pmatrix} 0 & -\frac{1}{2} \\ \frac{1}{2} & 0 \end{pmatrix}\begin{pmatrix} \frac{1}{4} & \frac{1}{2} \\ \frac{1}{2} & \frac{1}{4} \end{pmatrix}^{L-r-1}\Big] \tag{90}$$

This is easily calculated by using an orthogonal transformation

$$O\begin{pmatrix} \frac{1}{4} & \frac{1}{2} \\ \frac{1}{2} & \frac{1}{4} \end{pmatrix}O = \begin{pmatrix} \frac{3}{4} & 0 \\ 0 & -\frac{1}{4} \end{pmatrix}, \quad O\begin{pmatrix} 0 & -\frac{1}{2} \\ \frac{1}{2} & 0 \end{pmatrix}O = \begin{pmatrix} 0 & \frac{1}{2} \\ -\frac{1}{2} & 0 \end{pmatrix}, \quad O = \frac{1}{\sqrt{2}}\begin{pmatrix} 1 & 1 \\ 1 & -1 \end{pmatrix}. \tag{91}$$

We find a very nice, simple result

$$\langle \mathrm{GS}|S_1^z S_{r+1}^z|\mathrm{GS}\rangle = \Big(-\frac{1}{4}\Big)^r\Big(\frac{3}{4}\Big)^{L-r-1} + \Big(-\frac{1}{4}\Big)^{L-r}\Big(\frac{3}{4}\Big)^{r-1}. \tag{92}$$

Finally we take the normalization constant into account and then take the thermodynamic limit

$$\boxed{\lim_{L\to\infty}\frac{\langle \mathrm{GS}|S_1^z S_{r+1}^z|\mathrm{GS}\rangle}{\langle \mathrm{GS}|\mathrm{GS}\rangle} = 4\Big(-\frac{1}{3}\Big)^r = 4(-1)^r e^{-r\ln(3)}.} \tag{93}$$

This shows that in the ground state we have *short-range, antiferromagnetic correlations*:

- We have a finite correlation length $\xi = \frac{1}{\ln(3)} \approx 0.91$. This is less than one lattice spacing and therefore very short.

- The factor $(-1)^r$ tells us that neighbouring spins have a tendency to be anti-aligned.

- For large seprations $r \gg 1$ the correlations are vanishingly small, which in particular tells us that we do not have Néel order.

15

5.3 Hidden "string" order

We have seen in the previous subsection that the AKLT chain does not have antiferromagnetic long-range order, which is defined through the order parameter

$$\mathcal{O}_{\text{Néel}}^z = \lim_{|j-k|\to\infty} \lim_{L\to\infty} (-1)^{j-k} \frac{\langle \text{GS}|S_j^z S_k^z|\text{GS}\rangle}{\langle \text{GS}|\text{GS}\rangle} \ . \tag{94}$$

Our result (93) implies that $\mathcal{O}_{\text{Néel}}^z = 0$. Interestingly the AKLT has a different kind of "hidden" order. This is defined in terms of a so-called *string-order parameter*

$$\mathcal{O}_{\text{string}}^\alpha = \lim_{|j-k|\to\infty} \lim_{L\to\infty} \frac{\langle \text{GS}|S_j^\alpha e^{i\pi \sum_{\ell=j+1}^{k-1} S_\ell^z} S_k^\alpha|\text{GS}\rangle}{\langle \text{GS}|\text{GS}\rangle} \ , \qquad \alpha = x, y, z. \tag{95}$$

The string order parameter can be calculated in the same way as the spin-spin correlation functions (problem sheet 1). The numerator in the expression for $\mathcal{O}_{\text{string}}^z$ has a graphical representation shown in Fig. 5.3. Here
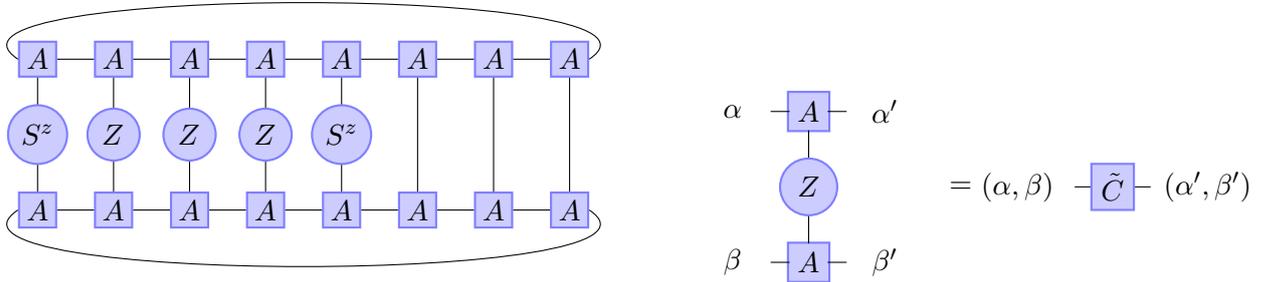
Figure 9: Graphical representation of the numerator in the expression for $\mathcal{O}_{\text{string}}^z$.

the 4×4 matrix $\tilde{C}$ is given by

$$\tilde{C} = \begin{pmatrix} \frac{1}{4} & -\frac{1}{2} & 0 & 0 \\ -\frac{1}{2} & \frac{1}{4} & 0 & 0 \\ 0 & 0 & -\frac{1}{4} & 0 \\ 0 & 0 & 0 & -\frac{1}{4} \end{pmatrix} , \quad \tilde{C}_{(\alpha\beta),(\alpha'\beta')} = \sum_{\sigma=+,0,-} A_{\alpha\alpha'}^\sigma A_{\beta\beta'}^\sigma \underbrace{\langle\sigma|e^{i\pi S^z}|\sigma\rangle}_{2\delta_{\sigma,0}-1}. \tag{96}$$

One finds that

$$\mathcal{O}_{\text{string}}^\alpha = \lim_{|j-k|\to\infty} \lim_{L\to\infty} \text{Tr}_{4\times4}\left[\tilde{B}\tilde{C}^{k-j-1}\tilde{B}\tilde{A}^{L-k+j-1}\right] = -\frac{4}{9}. \tag{97}$$

To get some physical intuiton about the string order parameter let us consider product states. Néel order would then correspond to configurations like $+-+-+-+-$. In contrast, the string order parameter would give an antiferromagnetic pattern *if we delete all sites where the spin is in the 0 state*, i.e. configurations like $+-0+0-+0000-+0-+000--+-$.

5.4 Bipartite entanglement entropy of matrix-product states

Consider a MPS of the form

$$|\Psi\rangle = \frac{1}{\mathcal{N}} \sum_{\sigma_1,\dots,\sigma_L} \text{Tr}\left[A^{\sigma_1}\dots A^{\sigma_L}\right] |\sigma_1,\dots,\sigma_L\rangle \ , \tag{98}$$

where $\mathcal{N}$ is a normalization factor and A are $\chi \times \chi$ matrices. We want to work out the bi-partite entanglement entropy of a sub-system consisting of the first ℓ sites. We will assume that the MPS is *injective*, which means that the matrices A^σ are such that

$$\sum_\sigma A^\sigma (A^\sigma)^\dagger = \lambda \mathbb{1} \ , \ \lambda > 0. \tag{99}$$

16

One can show that if this is the case then there existe a ℓ_0 such that for all $\ell > \ell_0$ the set of matrices $\{A^{\sigma_1} \ldots A^{\sigma_\ell}\}$ span the space of all $\chi \times \chi$ matrices. To work out the entanglement entropy we rewrite $|\Psi\rangle$ in the form

$$|\Psi\rangle = \frac{1}{\mathcal{N}} \sum_{\alpha,\beta=1}^{\chi} \underbrace{\sum_{\sigma_1,\ldots,\sigma_\ell} [A^{\sigma_1} \ldots A^{\sigma_\ell}]_{\alpha\beta} |\sigma_1,\ldots,\sigma_\ell\rangle}_{|\phi_{\alpha\beta}\rangle} \otimes \underbrace{\sum_{\sigma_{\ell+1},\ldots,\sigma_L} [A^{\sigma_{\ell+1}} \ldots A^{\sigma_L}]_{\beta\alpha} |\sigma_{\ell+1},\ldots,\sigma_L\rangle}_{|\psi_{\alpha\beta}\rangle} \tag{100}$$

We then assume that $\ell, L - \ell > \ell_0$, so that injectivity of the MPS implies that $\{|\phi_{\alpha\beta}\rangle\}$ and $\{|\psi_{\alpha\beta}\rangle\}$ both form sets of χ^2 linearly independent states. This means that there exist basis transformations U and V

$$|\tilde{\phi}_{\alpha\beta}\rangle = U|\phi_{\alpha\beta}\rangle \ , \quad |\tilde{\psi}_{\alpha\beta}\rangle = V|\psi_{\alpha\beta}\rangle \tag{101}$$

such that

$$\langle\tilde{\phi}_{\alpha'\beta'}|\tilde{\phi}_{\alpha\beta}\rangle = \delta_{\alpha,\alpha'}\delta_{\beta,\beta'} \ , \qquad \langle\tilde{\psi}_{\alpha'\beta'}|\tilde{\psi}_{\alpha\beta}\rangle = \delta_{\alpha,\alpha'}\delta_{\beta,\beta'}. \tag{102}$$

This provides us with a representation of our MPS of the form

$$|\Psi\rangle = \sum_{\alpha,\beta=1}^{\chi} \lambda_{\alpha\beta}|\tilde{\phi}_{\alpha\beta}\rangle \otimes |\tilde{\psi}_{\alpha\beta}\rangle \ , \qquad \sum_{\alpha,\beta=1}^{\chi} |\lambda_{\alpha\beta}|^2 = 1. \tag{103}$$

The reduced density matrix of the sub-system consisting of the first ℓ sites $[1, \ell]$ is then given by

$$\rho_{[1,\ell]} = \sum_{\alpha,\beta=1}^{\chi} |\lambda_{\alpha\beta}^2||\tilde{\phi}_{\alpha\beta}\rangle\langle\tilde{\phi}_{\alpha\beta}| \ . \tag{104}$$

This results in a bipartite entanglement entropy of

$$S_{[1,\ell]} = -\sum_{\alpha,\beta=1}^{\chi} |\lambda_{\alpha\beta}^2| \ln\left(|\lambda_{\alpha\beta}^2|\right) \le \ln\chi^2. \tag{105}$$

The final inequality derives from the fact that the entropy is always bounded by the dimension of the Hilbert space of states. This tells us that the entanglement entropy of a finite-dimensional MPS is always finite, i.e. does not scale with system size! This in turn implies that we cannot use MPS to approximate energy eigenstates at finite energy densities (as they display a volume law for the EE). On the other hand, MPS can be used very efficiently to approximate ground states and low-lying excitations of local Hamiltonians. The basic idea is to make a variational Ansatz in terms of an MPS, and then optimize the variational parameters, i.e. the matrices A^σ, to obtain the lowest possible energy. There are a number of different approaches such as the density matrix renormalization group (DMRG) and time-evolving block decimation (TEBD). Several codes are freely available online, e.g. https://www.itensor.org.

Part III

QUANTUM QUENCHES AND (GENERALIZED) THERMALIZATION

A *quantum quench* is a particular protocol for driving many-particle quantum system out of equilibrium. It is defined as follows.

1. The starting point of a many-particle system in a large, finite volume L with Hamiltonian H.

2. The system is then prepared in an initial state $|\Psi(0)\rangle$ that has non-zero overlaps with exponentially many (in system size) eigenstates of H. The initial state should have good clustering properties and is often taken to be a lowly entangled state.

3. At later times the quantum state describing the system is then given by the solution of the time-dependent Schrödinger equation

$$|\Psi(t)\rangle = e^{-iHt}|\Psi(0)\rangle. \tag{106}$$

4. The objective is to study expectation values of local operators $\mathcal{O}_A$ in the thermodynamic limit

$$\lim_{L\to\infty}\langle\Psi(t)|\mathcal{O}_A|\Psi(t)\rangle. \tag{107}$$

Here we define local operators as acting as the identity outside a finite, connected spatial region in the infinite volume limit. For a quantum spin chain operators of the form $\sigma_{j_1}^{\alpha_1}\ldots\sigma_{j_\ell}^{\alpha_\ell}$ where $j_k \in [a,b]$ with a,b fixed are local. As we will see later locality is a very important concept in non-equilibrium dynamics.

Often the Hamiltonian depends on a parameter h such a magnetic field or interaction strength, and a popular way of defining a quantum quench is then to take $|\Psi(0)\rangle$ as the ground state of $H(h_0)$, and consider time evolution under the Hamiltonian $H(h_1)$ with $h_1 \neq h_0$. This corresponds to an instantaneous "quench" of h at time $t = 0$ from h_0 to h_1.

For pedagogical reasons we restrict our discussion (with the exception of the next section) to

- Lattice models with finite local Hilbert spaces;

- Translationally invariant Hamiltonians;

- Translationally invariant initial states.

6 Quantum quenches and experiments

The theoretical quantum quench protocol introduced above is inspired by cold atom experiments. In order to make the connection more concrete I now present a brief cartoon of experiments on ultra-cold Rb atoms carried out in Jörg Schmiedmayer's group in Vienna, which have been the topic of previous lectures at this school. The Hamiltonian describing the atoms is to a good approximation

$$H(t) = \sum_j \left[-\frac{\hbar^2\nabla_j^2}{2m} + V(\boldsymbol{r}_j, t)\right] + \frac{g}{2}\sum_{j\neq k}\delta(\boldsymbol{r}_j - \boldsymbol{r}_k), \tag{108}$$

where $V(\boldsymbol{r}_j, t)$ is a confining potential that can be varied in a time-dependent way. The potential is separable in the sense that $V(\boldsymbol{r}_j, t) = V_\parallel(x_j, t) + V_\perp(y_j, z_j, t)$ and $V_\perp$ can be tuned in such a way that the transverse degrees of freedom are essentially projected to the ground state(s) of the single-particle Hamiltonian

$$H_{\perp,0} = \sum_j -\frac{\hbar^2}{2m}\left[\frac{\partial^2}{\partial y_j^2} + \frac{\partial^2}{\partial z_j^2}\right] + V_\perp(y_j, z_j, t). \tag{109}$$

By choosing the transverse confining potential to be very tight and having a single minimum the system at time $t = 0$ can be prepared in a low temperature thermal state of the one dimensional Hamiltonian

$$H(0) \approx \sum_j \left[-\frac{\hbar^2}{2m}\frac{\partial^2}{\partial x_j^2} + \frac{1}{2}m\omega_\parallel^2 x_j^2\right] + c\sum_{j<k}\delta(x_j - x_k). \tag{110}$$

In the experiments $V_\perp(y_j, z_j, t)$ is then changed in a time-dependent fashion so that one ends up with a tight double-well potential in the transverse direction. Neglecting the higher transverse modes (as they have very high energies) then leads to a Hamiltonian that in second quantization takes the form

$$H(t_0) \approx \int dx \sum_a \left[\Psi_a^\dagger(x) \left(-\frac{1}{2m}\frac{d^2}{dx^2} + \frac{m\omega_\parallel^2}{2}x^2 \right) \Psi_a(x) + g\Psi_a^\dagger(x)\Psi_a^\dagger(x)\Psi_a(x)\Psi_a(x) \right]. \tag{111}$$

Here $a = 1, 2$ label the two wells, *cf.* Fig. 6. The splitting process leaves the system in some initial state

$t = 0\,\mathrm{ms}$ $t = 6\,\mathrm{ms}$
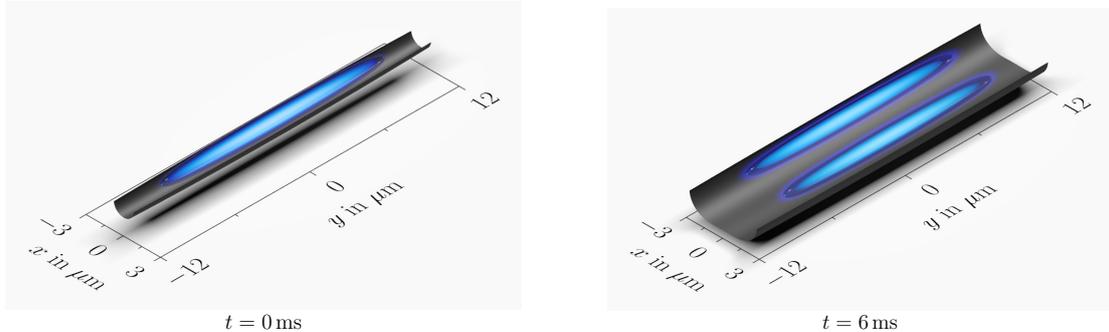
Figure 10: By changing the transverse confining potential a one dimensional Bose gas is "split into two".

$|\Psi(t_0)\rangle$ that is not an eigenstate of $H(t_0)$: in this sense the situation is analogous to a quantum quench. The system is now left to evolve in time governed by the Hamiltonian (111). At a time t_1 the confining potential is switched off and the two clouds of atoms start to expand freely in three dimensions. Eventually they overlap and at a time t_2 the density of atoms is measured. The expansion can be easily modelled
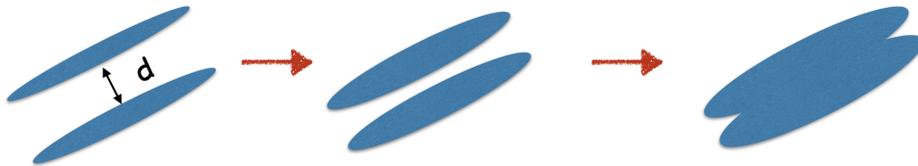
Figure 11: After switching off the confining potential the atomic clouds expand in three dimensions and eventually overlap.

as the atoms effectively do not interact. One therefore can integrate the Heisenberg equations of motion for the measured observable (the particle density) backwards and relate it to an operator in the split one dimensional Bose gas at time t_1. One finds that the measured density is

$$\rho_{\mathrm{tof}}(x, \mathbf{r}, t_2) \approx \sum_{a,b=1}^{2} g_{ab}(t_2 - t_1, \mathbf{r})\Psi_a^\dagger(x, t_1)\Psi_b(x, t_1) , \tag{112}$$

where $\mathbf{r}$ denote the transverse directions and $g_{ab}(t, \mathbf{r})$ are known functions. Repeating the experiment many times then provides access to e.g. the expectation value (112) in the split, one-dimensional Bose gas after a period of non-equilibrium evolution.

7 Local relaxation

The first question to ask is whether after a quantum quench a many-particle system somehow relaxes, i.e. whether if we wait long enough the quantum mechanical probability distributions describing the outcomes

19

of measurements become time independent. This is equivalent to the question whether the double limit

$$\lim_{t \to \infty} \lim_{L \to \infty} \langle \Psi(t) | \mathcal{O} | \Psi(t) \rangle \tag{113}$$

exists for all Hermitian operators $\mathcal{O}$. We note that the order of limits is crucial here. It is easy to see that this limit cannot exist for all observables. Indeed, let $|n\rangle$ be the eigenstates of the Hamiltonian describing the time evolution of our system and E_n the corresponding energies. Then

$$|\Psi(t)\rangle = \sum_n e^{-iE_n t} \langle n | \Psi(0) \rangle \, |n\rangle. \tag{114}$$

Now we can choose "observables" that never relax, e.g.

$$\mathcal{O} = \mathcal{O}^\dagger = |1\rangle\langle 2| + |2\rangle\langle 1|. \tag{115}$$

Indeed, we have

$$\langle \Psi(t) | \mathcal{O} | \Psi(t) \rangle = A \cos\big((E_1 - E_2)t + \varphi\big), \tag{116}$$

which shows that the expectation value of this particular observables is a periodic function of time. However, the operator $\mathcal{O}$ is highly non-local. This suggests that we should restrict our attention to *local measurements* and concomitantly *local operators* $\mathcal{O}_A$. For these our double limit generally exists, i.e.

$$\lim_{t \to \infty} \lim_{L \to \infty} \langle \Psi(t) | \mathcal{O}_A | \Psi(t) \rangle = \langle \mathcal{O}_A \rangle_{\text{stat}}. \tag{117}$$

The physical picture underlying this fact is as follows. As $\mathcal{O}_A$ is a local operator it acts like the identity outside some finite spatial region A. In the infinite volume limit the complement of A simply acts like a bath on A and eventually leads to relaxation. One can reformulate this observation in terms of density matrices as follows. The density matrix of the entire system $\rho(t) = |\Psi(t)\rangle\langle\Psi(t)|$ in our case is a pure state and hence can never relax. On the other hand, the *reduced density matrix*

$$\rho_A(t) = \text{Tr}_{\bar{A}}\big[\rho(t)\big] \tag{118}$$

describing the region A on which our observable acts ($\bar{A}$ is the complement of A) is a mixed state and hence can become time-independent at late enough times.

A natural question to ask at this point whether it is possible to describe the late-time limits of the expectation values of local operators in terms of a statistical ensemble. In other words, is it possible to find a time-independent density matrix ρ_{SS} such that for any local operator

$$\lim_{t \to \infty} \lim_{L \to \infty} \langle \Psi(t) | \mathcal{O}_A | \Psi(t) \rangle = \lim_{L \to \infty} \text{Tr}\big[\rho_{\text{SS}} \mathcal{O}_A\big]. \tag{119}$$

We note that in analogy to equilibrium statistical mechanics (where we can choose from micro-canonical, canonical and grand canonical ensembles) ρ_{SS} is not unique.

7.1 Local Conservation Laws

A *local conservation law* is a Hermitian operator $I^{(n)}$ that commutes with the Hamiltonian of our system and has a density $I_j^{(n)}$ that is a local operator as defined above, i.e.

$$I^{(n)} = \sum_j I_j^{(n)} \, , \quad [H, I^{(n)}] = 0. \tag{120}$$

We stress that the conservation laws we have in mind here are extensive. The existence of a local conservation law has important consequences for the steady state density matrix ρ_{SS} in translationally invariant cases. By (120) we have

$$\langle \Psi(t) | I^{(n)} | \Psi(t) \rangle = \text{time independent}. \tag{121}$$

Translational invariance then implies that

$$\lim_{L \to \infty} \frac{1}{L} \sum_j \langle \Psi(t) I_j^{(n)} | \Psi(t) \rangle = \lim_{L \to \infty} \langle \Psi(t) I_j^{(n)} | \Psi(t) \rangle. \tag{122}$$

Combining (122) with (121) we conclude that

$$\lim_{L \to \infty} \langle \Psi(0) I_j^{(n)} | \Psi(0) \rangle = \lim_{t \to \infty} \lim_{L \to \infty} \langle \Psi(t) I_j^{(n)} | \Psi(t) \rangle = \mathrm{Tr}\left[\rho_{\mathrm{SS}} \ I_j^{(n)} \right], \tag{123}$$

where in the last step we have used that $I_j^{(n)}$ are local operators. This tells us that ρ_{SS} *retains information about the expectation values of local conservation laws in the initial state.*

7.2 Thermalization

As we are dealing with an isolated quantum system energy is always conserved

$$e_0 = \lim_{L \to \infty} \frac{\langle \Psi(t) | H | \Psi(t) \rangle}{L}. \tag{124}$$

This is the minimal amount of information on the initial state $|\Psi(0)\rangle$ that gets retained under the dynamics. If there are no conserved quantities other than energy the system *thermalizes* at late times after a quantum quench. The steady state density matrix is then given by a finite temperature (equilibrium) ensemble constructed as follows. We define a Gibbs density matrix

$$\rho_{\mathrm{GE}} = \frac{e^{-\beta_{\mathrm{eff}} H}}{Z_{\mathrm{GE}}}, \tag{125}$$

and fix the effective temperature $\beta_{\mathrm{eff}}^{-1}$ by requiring it to correspond to the energy density established by the choice of initial state

$$e_0 = \lim_{L \to \infty} \frac{\mathrm{Tr}\left[\rho_{\mathrm{GE}} \ H \right]}{L}. \tag{126}$$

Under this choice we have

$$\rho_{\mathrm{SS}} = \rho_{\mathrm{GE}} . \tag{127}$$

We could have equally well chosen a micro-canonical description

$$\rho_{\mathrm{SS}} = \rho_{\mathrm{MC}} = \sum_{|E_n - Le| < \epsilon} |n\rangle\langle n|, \tag{128}$$

where $|n\rangle$ are energy eigenstates with energy E_n. Finally we note that averaging over a micro-canonical shell is not required as long we use a typical energy eigenstate to define our micro-canonical ensemble, which then takes the simple form

$$\rho_{\mathrm{MC}} = |n\rangle\langle n| . \tag{129}$$

Drawing an energy eigenstate at random out of our micro-canonical window provides us with a typical state with a probability that is exponentially close (in L) to one.

7.3 Non-equilibrium steady states and Generalized Gibbs Ensembles

If we have additional conservation laws with local densities $I_j^{(n)}$ the system cannot thermalize because

$$\lim_{L \to \infty} \langle \Psi(0) I_j^{(n)} | \Psi(0) \rangle = \mathrm{Tr}\left[\rho_{\mathrm{SS}} \ I_j^{(n)} \right], \tag{130}$$

which tells us that the system retains more information on the initial state than just its energy density. What should the ensemble describing the steady state then be? The answer to this question is provided

by Jaynes and Rigol et al: we should maximize the entropy under the constraints (130). This leads to a *generalized Gibbs ensemble*

$$\rho_{\text{GGE}} = \frac{1}{Z_{\text{GGE}}} e^{-\sum_n \lambda_n I^{(n)}}, \tag{131}$$

where the Lagrange multipliers λ_n are fixed by

$$\lim_{L \to \infty} \langle \Psi(0) I_j^{(n)} | \Psi(0) \rangle = \text{Tr} \left[\rho_{\text{GGE}} \, I_j^{(n)} \right]. \tag{132}$$

We note that solving these equations is a difficult task in general.

7.4 A simple explicit example

It is useful to make the above discussion concrete by considering a simple explicit example. We take as our Hamiltonian a one-dimensional tight-binding model of spinless fermions

$$H = -J \sum_{j=1}^{L} c_j^\dagger c_{j+1} + c_{j+1}^\dagger c_j \; . \tag{133}$$

This can be diagonalized by going to momentum space

$$c(k_n) = \frac{1}{\sqrt{L}} \sum_{j=1}^{L} e^{ik_n j} c_j \; , \qquad k_n = \frac{2\pi n}{L}. \tag{134}$$

We have

$$H = \sum_n \epsilon(k_n) \, c^\dagger(k_n) c(k_n) \; , \quad \epsilon(k) = -2J\cos(k). \tag{135}$$

As our initial state we choose

$$|\Psi(0)\rangle = \prod_{j=1}^{L/2} c_{2j}^\dagger |0\rangle \; , \tag{136}$$

where $c_j|0\rangle = 0$. The time evolved annihilation operators in the Heisenberg picture are obtained by solving the Heisenberg equations of motion

$$c(k_n, t) = e^{-it\epsilon(k_n)} c(k_n) \; . \tag{137}$$

The equal-time single-particle Green's function in momentum space is thus

$$\langle \Psi(0) | c^\dagger(k, t) c(p, t) | \Psi(0) \rangle = e^{it[\epsilon(k) - \epsilon(p)]} \frac{\delta_{k,p} + \delta_{k,p \pm \pi}}{2} \; . \tag{138}$$

This oscillates indefinitely in time and does not relax in any way. This is not a problem because $c^\dagger(k,t)c(p,t)$ is not a local operator. On the other hand, in position space we have

$$g_{j,k}(t) = \langle \Psi(0) | c_j^\dagger(t) c_k(t) | \Psi(0) \rangle = \frac{1}{2} \delta_{j,k} + \frac{(-1)^j}{2L} \sum_p e^{-ip(k-j) + 4iJt\cos(p)}$$

$$\to \frac{\delta_{j,k}}{2} + \frac{(-1)^j}{2} i^{|j-k|} J_{|j-k|}(4Jt), \tag{139}$$

where in the last line we have taken $L \to \infty$. At late times and fixed j, k this has the following asymptotic behaviour

$$g_{j,k}(t) = \frac{\delta_{j,k}}{2} + \frac{(-1)^j}{2} i^{|j-k|} \frac{1}{\sqrt{2\pi Jt}} \cos\left(4Jt - \frac{|j-k|\pi}{2} - \frac{\pi}{4}\right) + \mathcal{O}(t^{-1}). \tag{140}$$

This exhibits local relaxation in a power-law fashion to a stationary value of $\delta_{j,k}/4$. By Wick's theorem this implies that any local observable relaxes in a power-law fashion, e.g.

$$\langle \Psi(t) | c_j^\dagger c_k^\dagger c_l c_m | \Psi(t) \rangle = g_{j,m}(t) g_{k,l}(t) - g_{j,l}(t) g_{k,m}(t) \; . \tag{141}$$

22

The ensemble describing the stationary state is defined through the requirements that Wick's theorem should hold and

$$\lim_{t\to\infty} \lim_{L\to\infty} g_{j,k}(t) = \frac{\delta_{j,k}}{2} = \mathrm{Tr}\left[\rho_{\mathrm{SS}} \; c_j^\dagger c_k\right]. \tag{142}$$

We can choose ρ_{SS} as an infinite temperature Gibbs ensemble

$$\rho_{\mathrm{SS}} = \frac{1}{2^L}\mathbb{1} \; . \tag{143}$$

Given the fact that the tight-binding model is integrable and has an extensive number of local conservation laws (see below) according to our discussion above the steady state density matrix should be described by a generalized Gibbs ensemble. This is in fact correct, but it turns out that this GGE is identical to a simple Gibbs ensemble. Our results for the single-particle Green's function allow us to exhibit another interesting property of relaxation after quantum quenches. To that end we consider the particle density $n_j = c_j^\dagger c_j$

$$\langle\Psi(t)|n_j|\Psi(t)\rangle = \langle\Psi(0)|n_j(t)|\Psi(0)\rangle = \frac{1}{2} + \frac{(-1)^j}{2}J_0(4Jt). \tag{144}$$

We plot the resulting density as a function of time for even and odd sublattices in Fig. 7.4. At early
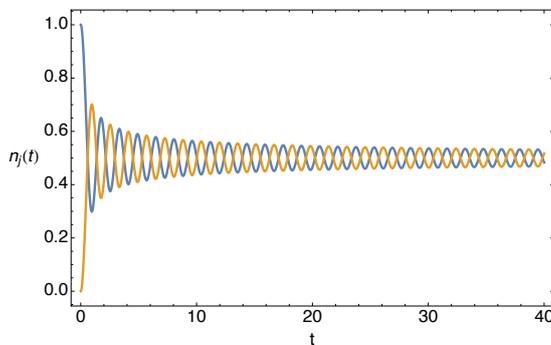
Figure 12: Density on even/odd sublattices after a quantum quench from the state (136).

times we clearly see the charge-density wave order of the initial state (136), which breaks translational invariance by one site. However, at late times this order "melts" and in the steady state the particle density is homogeneous. This shows that full translational invariance is restored in the steady state. Such symmetry restoration is a generic feature of quantum quenches in one-dimensional systems.

8 Spreading of correlations

Starting with the seminal work by Calabrese and Cardy [1, 2] the spreading of entanglement and correlations after quantum quenches has been explored in great detail. In the following we exhibit some of the important findings for our specific example of a quench from a CDW state in the tight-binding model. The connected density-density correlation for that problem is easily obtained using Wick's theorem. In the thermodynamic limit it reads

$$D_{j,j+\ell}(t) = \langle\Psi(0)|n_j(t)n_{j+\ell}(t)|\Psi(0)\rangle_c = \frac{\delta_{\ell,0}}{4} - \frac{1}{4}J_{|\ell|}^2(4Jt). \tag{145}$$

The result is shown in Fig. 8. We see that for a given separation ℓ the connected correlator is very small until a time

$$t = \frac{|\ell|}{2v_{\max}} \; , \quad v_{\max} = \max_p \frac{d\epsilon(p)}{dp} = 2J. \tag{146}$$

After that time significant connected correlations are observed. This behaviour is generic for integrable models and is referred to as a "light-cone" effect. Some remarks are in order:
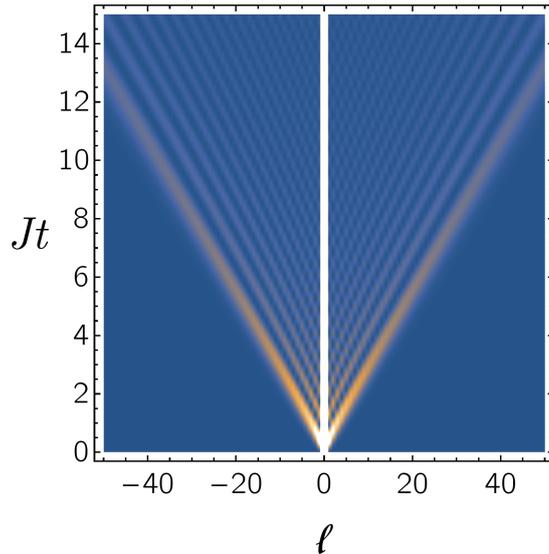
Figure 13: Connected density-density correlation function $D_{j,j+\ell}(t)$ for the tight-binding model on the infinite chain as a function of ℓ and t for $j = 1$ after a quantum quench from the state (136).

- If the correlation length in the initial state $|\Psi(0)\rangle$ is finite (as in our example) the light-cone effect is very pronounced.

- If the correlation length in the initial state $|\Psi(0)\rangle$ is infinite there still is a light-cone effect, but it is much weaker [3, 4].

- For long-range interactions the light-cone effect is different [5].

8.1 Light-cone effect vs operator spreading

It is instructive to connect the light-cone effect to *operator spreading*. The Heisenberg operators $c_j(t)$ act non-trivially on the entire system for any $t > 0$. This can be seen e.g. by expanding

$$c_j(t) = e^{iHt} c_j e^{-iHt} = c_j - it[H, c_j] - \frac{t^2}{2}[H, [H, c_j]] + \ldots \tag{147}$$

However, the contributions to $c_j(t)$ are very small outside a light-cone. This can be seen by using the Heisenberg equation of motion

$$c_j(t) = \frac{1}{\sqrt{L}} \sum_p e^{-ipj} c(p, t) = \sum_\ell c_\ell \frac{1}{L} \sum_p e^{ip(\ell-j) - i\epsilon(p)t} \simeq \sum_\ell (i)^{|\ell-j|} J_{|\ell-j|}(2Jt) \, c_\ell. \tag{148}$$

The amplitudes $J_l(2Jt)$ are plotted in Fig. 8.1. We see that $J_l(2Jt)$ becomes very small for $l > 2Jt = v_{\max}t$. This means that $c_j(t)$ can be accurately approximated by an operator $\widetilde{c}_j(t)$ that acts non-trivially only on a finite interval $[j - v_{\max}t, j + v_{\max}t]$. This in turn tells us that the density operators $n_j(t)$ can be well approximated by $\widetilde{n}_j(t)$ that act as the identity outside $[j - v_{\max}t, j + v_{\max}t]$ and establishes the picture for operator growth shown in Fig. 8.1. Using that fact for short enough times $t < |\ell|/2J$ the operators $\widetilde{n}_j(t)$ and $\widetilde{n}_{j+\ell}(t)$ act on different parts of our system and our initial state $|\Psi(0)\rangle$ is a product state we conclude that

$$\langle \Psi(0)|n_j(t)n_{j+\ell}(t)|\Psi(0)\rangle \approx \langle \Psi(0)|n_j(t)|\Psi(0)\rangle\langle \Psi(0)|n_{j+\ell}(t)|\Psi(0)\rangle, \ t < |\ell|/2J. \tag{149}$$

This accounts for the light-cone effect seen in Fig. 8.

24
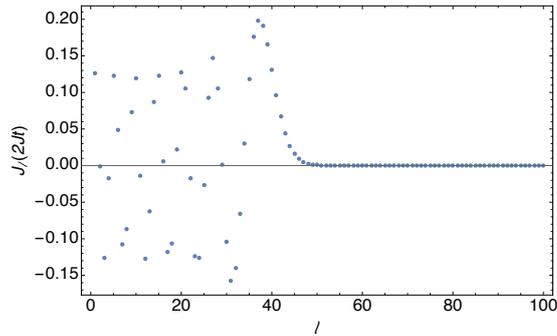
Figure 14: $J_l(2Jt)$ as a function of l for $Jt = 20$.
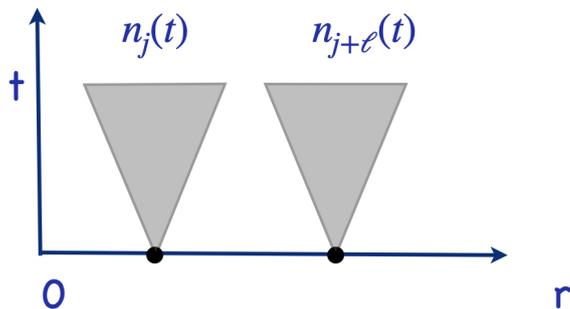
Figure 15: Space-time plot of the effective size of the Heisenberg picture operators $n_j(t)$ and $n_{j+\ell}(t)$.

8.2 Relation to Lieb-Robinson bound

Our discussion on operator spreading relied on the fact that in our example the Heisenberg equations of motion are linear and can be solved exactly. However, there are rigorous results on operator spreading that lift the picture we have just established, to a certain extent, to quantum quenches in general. For non-relativistic quantum spin systems with short-ranged Hamiltonians the *Lieb-Robinson bound* provides a bound for the norm of the commutator of two operators that at time $t = 0$ act respectively only on spins inside two spatially separated regions A and B, *cf.* Fig. 8.2. Lieb and Robinson proved that [6, 7]
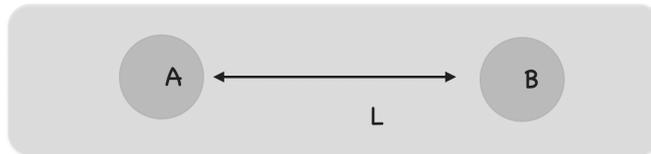
Figure 16: Setup for the Lieb-Robinson bound: two operators initially act only on spins in regions A and B that are spatially separated by a distance L.

$$\|[\mathcal{O}_A(t), \mathcal{O}_B(0)]\| \leq c \min(|A|, |B|) \|\mathcal{O}_A\| \|\mathcal{O}_B\| e^{-\frac{L-vt}{\xi}} . \tag{150}$$

Here $\|.\|$ denotes the operator norm, $|A|$ and $|B|$ are respectively the numbers of sites in regions A and B and v, c, ξ are constants. The Lieb-Robinson bound implies that the operator $\mathcal{O}_A(t)$ can be well approximated

by an operator that acts only on spins in the interior of the (forward) light-cone of region A [8]. This is completely analogous to what we just discussed for free theories! This fact is sufficient to show that for initial states $|\Psi(0)\rangle$ with finite correlation lengths one has [8]

$$\langle\Psi(0)|\mathcal{O}_A(t)\mathcal{O}_B(t)|\Psi(0)\rangle_c < \bar{c}(|A|+|B|)\, e^{-\frac{L-2vt}{\chi}} \,, \tag{151}$$

where $\bar{c}$, v and χ are constants and L is the separation between regions A and B. This establishes the existence of a "speed limit" for *sizeable* connected correlations to emerge, in perfect agreement with the light-cone effect observed after quantum quenches. Some comments are in order:

- The Lieb-Robinson bound is a statement about operators and is independent of which quantum state the system is in. This means in particular that the "Lieb-Robinson velocity" v is not necessarily related to any observed "light-cone velocity", because the latter is in general state-dependent [9].

- As the name suggests, the Lieb-Robinson bound is a bound and does not imply that there will be a visible light-cone effect.

8.3 Calabrese-Cardy quasi-particle picture

There is a very nice physical picture that explains light-cone effects in the spreading of correlations and entanglement due to Calabrese and Cardy [1, 2], *cf.* Fig. 8.3.
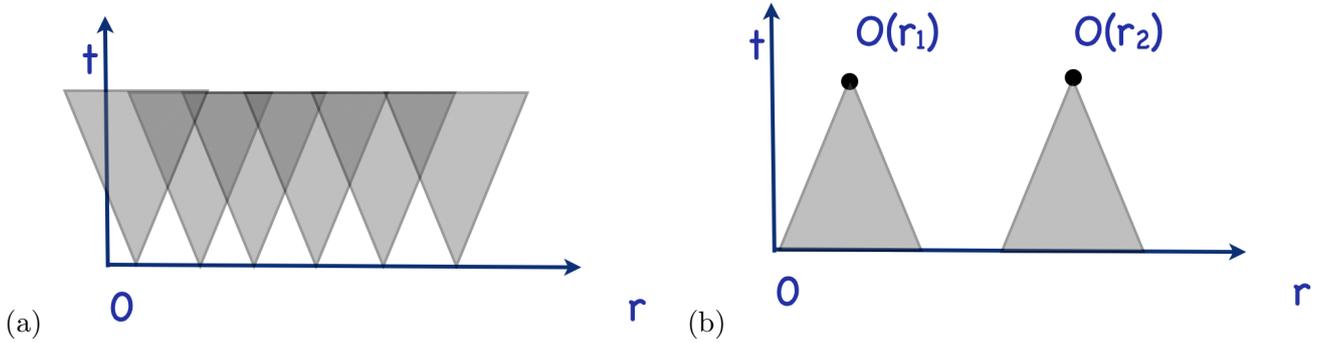
Figure 17: Quasi-particle picture for light-cone effects in the spreading of correlations and entanglement.

- The quantum quench creates quasi-particles at time $t = 0$, which start propagating with velocities $|v| \leq v_{\max}$, *cf.* Fig. 8.3 (a).

- At short times $t > 0$ operators at positions $r_{1,2}$ are "hit" by quasi-particles emanating from within their backwards light-cones, *cf.* Fig. 8.3 (b). This leads to a dephasing of one-point functions, but connected correlations remain small.

$$\langle\Psi(0)|\mathcal{O}(r_1,t)\mathcal{O}(r_2,t)|\Psi(0)\rangle \approx \langle\Psi(0)|\mathcal{O}(r_1,t)|\Psi(0)\rangle\,\langle\Psi(0)|\mathcal{O}(r_2,t)|\Psi(0)\rangle. \tag{152}$$

- At a time $t^* = |r_2-r_1|/2v_{\max}$ the two backwards light-cones touch and (sizeable) connected correlations develop.

Light-cone effects have been studied in cold-atom experiments, see e.g. [10, 11]. The experiments of Ref. [10] correspond to an interaction quench for a system of lattice bosons with Hamiltonian

$$H = -J\sum_j a_j^\dagger a_{j+1} + a_{j+1}^\dagger a_j + \frac{U}{2}\sum_j n_j(n_j-1)\,. \tag{153}$$

The system is prepared in an initial state $|\Psi(0)\rangle$ and by changing the optical lattice potential the ratio U/J is then quenched from about 40 to 9. The system is let to evolve in time and eventually an "occupation parity" two-point function is measured

$$C_d(t) = \langle\Psi(0)|s_j(t)\ s_{j+d}(t)|\Psi(0)\rangle_c\ , \tag{154}$$

where $s_j = 1$ ($s_j = -1$) if site j is occupied by an odd (even) number of bosons. The measurements show a clear light-cone effect.

9 Finite-size effects

In the above we have stressed the importance of taking the thermodynamic limit before considering the late time behaviour. Indeed, the thermodynamic and late time limits do not commute. However, experimental systems are of course all finite (and often not even particularly large) and it is therefore important to understand how the above considerations are modified for quantum quenches in finite systems. Working with a finite system has two obvious consequences:

- Local relaxation in the sense discussed above is impossible.

- There are finite-size effects in the dynamics at finite times.

9.1 Relaxation of time averages and diagonal ensemble

To address the issue of relaxation in finite systems it is customary to consider time averages

$$\bar{\mathcal{O}}_T = \frac{1}{T}\int_0^T dt\langle\Psi(t)|\mathcal{O}|\Psi(t)\rangle\ . \tag{155}$$

Relaxation then corresponds to the existence of the limit $\lim_{T\to\infty}\bar{\mathcal{O}}_T$. The physical picture is that the expectation value keeps on fluctuating around its late-time average, but for most of the time is found very close to the latter.

Late-time averages can be described by the so-called *diagonal ensemble*. The idea is to expand the time evolved state $|\Psi(t)\rangle$ in energy eigenstates $|n\rangle$

$$\bar{\mathcal{O}}_T = \sum_{n,m}\frac{1}{T}\int_0^T dt\langle\Psi(0)|n\rangle\langle n|\mathcal{O}|m\rangle\langle m|\Psi(0)\rangle\ e^{-it(E_m-E_n)}. \tag{156}$$

Assuming for simplicity that the energy spectrum is non-degenerate we have

$$\lim_{T\to\infty}\bar{\mathcal{O}}_T = \sum_n |\langle\Psi(0)|n\rangle|^2\langle n|\mathcal{O}|n\rangle\ . \tag{157}$$

This only involves diagonal matrix elements of $\mathcal{O}$ in the basis of energy eigenstates and is therefore known as *diagonal ensemble*. It is believed that for local observables the infinite time average coincides with the stationary value in the thermodynamic limit up to finite-size corrections, i.e.

$$\lim_{T\to\infty}\bar{\mathcal{O}}_T = \lim_{t\to\infty}\lim_{L\to\infty}\langle\Psi(t)|\mathcal{O}|\Psi(t)\rangle + o(L^0)\ . \tag{158}$$

For this to be true, the diagonal ensemble must be able to describe thermal states. At first sight this seems very strange, because (158) looks like it should be very sensitive to the precise form of the initial state $|\Psi(0)\rangle$, whereas the stationary state density matrix of a thermal ensemble only "remembers" its energy density.Let us recall that the Hamiltonians we are interested in have densities $H = \sum_j H_j$ that are short-ranged and that our initial state $|\Psi(0)\rangle$ is assumed to have good clustering properties. In this case there are two ingredients in establishing that the diagonal ensemble can describe thermal states.

1. Firstly, the overlaps $|\langle\Psi(0)|n\rangle|$ become very strongly peaked in energy for large system sizes L. To see this we first note that the average energy is extensive $\bar{E} = \langle\Psi(0)|H|\Psi(0)\rangle = eL$. The variance can be expressed as

$$(\Delta E)^2 = \langle\Psi(0)|H^2|\Psi(0)\rangle - \langle\Psi(0)|H|\Psi(0)\rangle^2$$
$$= \sum_{n,m}\langle\Psi(0)|H_n H_m|\Psi(0)\rangle_c. \tag{159}$$

Using that $|\Psi(0)\rangle$ has good clustering properties and that H_n are local operators we can conclude that the connected correlation functions vanish for large $|n-m|$. This implies that

$$(\Delta E)^2 \propto L^\alpha , \quad \alpha < 2. \tag{160}$$

Hence

$$\frac{(\Delta E)^2}{\bar{E}^2} \propto L^{\alpha-2} . \tag{161}$$

This establishes that for large L the probability distribution of energy and hence $|\langle\Psi(0)|n\rangle|$ is strongly peaked.

2. According to the Eigenstate Thermalization Hypothesis (see below) the expectation values of local operators in nearby typical energy eigenstates away from the edges of the spectrum fulfil

$$\langle n|\mathcal{O}|n\rangle = g_\mathcal{O}(E_n) , \tag{162}$$

where $g_\mathcal{O}$ is a smooth function of energy (and for $L \to \infty$ becomes a smooth function of energy density).

Combining these two ingredients we have for $E_k = eL + \mathcal{O}(L^0)$

$$\lim_{T\to\infty}\bar{\mathcal{O}}_T = \sum_n |\langle\Psi(0)|n\rangle|^2\langle n|\mathcal{O}|n\rangle \approx \langle k|\mathcal{O}|k\rangle \sum_n |\langle\Psi(0)|n\rangle|^2 = \langle k|\mathcal{O}|k\rangle. \tag{163}$$

In this way the diagonal ensemble can reproduce the micro-canonical ensemble.

9.2 Traversals and revivals

We now turn to some generic finite-size effects. Let us start by considering the density-density correlator $D_{j,j+\ell}(t)$ (145) in our example of a quantum quench in the tight-binding model, but now on a finite ring of $L = 64$ sites. The results are shown in Fig. 9.2. For convenience we reproduce the result in the thermodynamic limit on the left. We observe pronounced differences between the results in the infinite and finite volume at fairly short times. The most striking effect is related to the light-cone in the connected correlation function traversing the ring. Concomitantly this effect has been termed a *traversal*. If we consider a fixed separation $0 < \ell < L/2$ between our two density operators, the light cone arrives at the time $t_\ell^* = \ell/2v_{\max}$ and sizeable connected correlations develop. At the later time

$$t_\ell = \frac{L-\ell|}{2v_{\max}} \tag{164}$$

a signal from the "traversed light cone" appears. The next traversal occurs at time $(L+\ell)/2v_{\max}$ and so on. Traversals are a simple geometric effect (and occur for open chains as well) and on time scales that scale linearly in system size. They are very different from *revivals*, which can be defined as instances when the return amplitude becomes large, i.e. the time evolved quantum state has a large overlap with the initial state

$$R(t) = |\langle\Psi(t)|\Psi(0)\rangle| \sim 1. \tag{165}$$

(a)   (b)
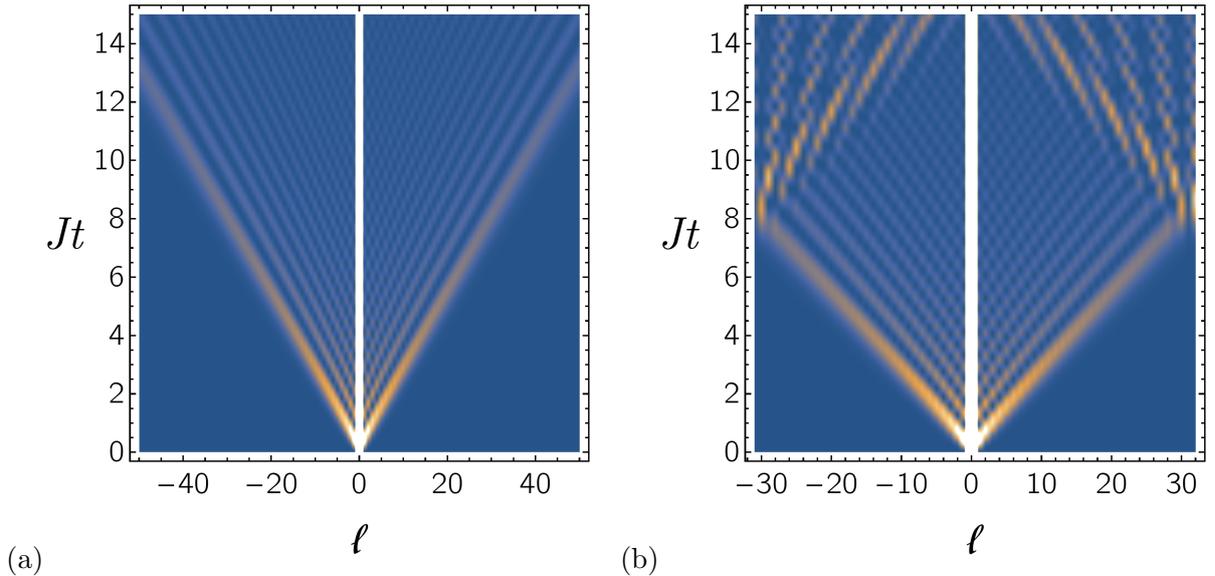
Figure 18: Connected density-density correlation function $D_{j,j+\ell}(t)$ for a quench from a CDW product state in the tight-binding model 7.4. Results are shown in the thermodynamic limit (a) and on a ring of 64 sites (b).
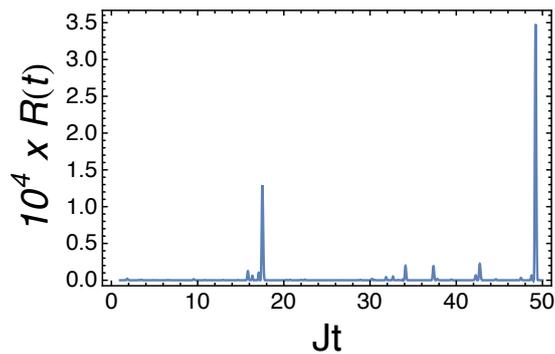
Figure 19: Magnitude of the return amplitude after a quench from a CDW product state in the tight-binding model 7.4 for a system of $L = 64$ sites.

In our example the return amplitude is in fact tiny as shown in Fig. 9.2. Unlike traversals revivals are related to regularities in the spectrum of the Hamiltonian, see e.g. [12]. Expanding the return amplitude in a basis of energy eigenstates we have

$$R(t) = \left| \sum_n |\langle \Psi(0)|n\rangle|^2 e^{iE_n t} \right|. \tag{166}$$

For a lattice spin system with finite dimensional local Hilbert space we have a finite number of energy eigenvalues that can be approximated to any desired precision by rational numbers. Hence we can always find a time t^* such that

$$E_n t^* \approx 0 \bmod 2\pi \ \forall n. \tag{167}$$

At this revival time we have $R(t) \approx 1$. Importantly, for many-particle systems revival times are typically extremely large and only become small if the energy spectrum is highly regular. An example is the spinless

fermion Hamiltonian

$$H = -J \sum_{j=1}^{L} \sum_{n=0}^{N} \frac{1}{(2n+1)^2} \left[c_j^\dagger c_{j+2n+1} + \text{h.c.} \right] = \sum_p \epsilon_N(p) \, c^\dagger(p) c(p) \ . \tag{168}$$

By taking N large enough we can make the dispersion relation approximately linear, *cf.* Fig. 9.2 (a). This in turn leads to a very regular many-particle spectrum with an approximately equal spacing of $2\pi v/L$, where v is the velocity and L the system size. As a result the revival time scales linearly in system size. In Fig. 9.2

(a)

(b)
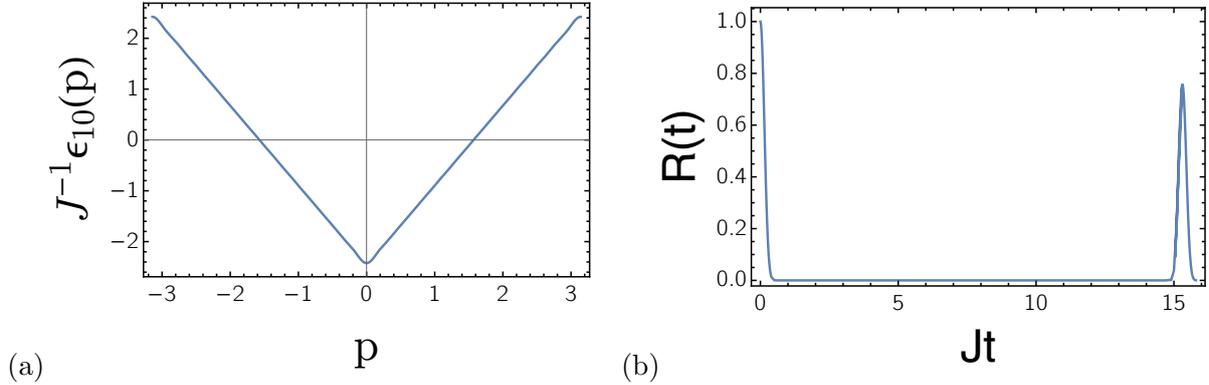
Figure 20: Magnitude of the return amplitude after a quench from a CDW product state in the tight-binding model 7.4 for a system of $L = 48$ sites.

we plot the magnitude of the return amplitude after a quantum quench to the model (168) as a function of time. A revival is seen to occur at a time $t^* \approx 15/J$. The fact that this occurs at around half the time expected on the basis of the level spacing is related to our particular choice of initial state. Revivals have been observed in cold atom experiments with highly regular spectra [13].

10   Eigenstate Thermalization Hypothesis (ETH)

The ETH is a conjecture on what the matrix elements of local Hermitian operators in energy eigenstates of generic [1], local Hamiltonians look like [14]. Let $H|n\rangle = E_n|n\rangle$, L be the volume of our system, and $\mathcal{O}$ a local, Hermitian operator. Then the ETH states that

$$\boxed{\langle m|\mathcal{O}|n\rangle = g_\mathcal{O}(\bar{E})\delta_{n,m} + e^{-\frac{1}{2}S(\bar{E})} f_\mathcal{O}(\bar{E},\omega) R_{n,m} \ , \quad \bar{E} = \frac{E_n + E_m}{2} \ , \quad \omega = E_n - E_m,} \tag{169}$$

where

- $g_\mathcal{O}(x)$ is a smooth function of x;

  This implies that for large system sizes diagonal matrix elements are approximately smooth functions of the *energy density*, which fits nicely with our previous discussion of the micro-canonical ensemble.

- $f_\mathcal{O}(x,y)$ is a smooth function of x and y;

  Note that the function $f_\mathcal{O}(x,y)$ can in principle be very small itself – for example it is allowed to become vanishingly small unless $y/L = o(L^0)$.

- $S(\bar{E})$ is the thermodynamic entropy at energy $\bar{E}$;

  As the entropy at finite energy densities in (typically) extensive, off-diagonal MEs are exponentially small in system size.

---

[1]This means that there are no local conservation laws other than energy and particle number.

- $R_{n,m} = R_{m,n}^*$ are random variables with zero mean and unit variance, i.e.

$$\overline{R_{n,m}} = 0 \ , \qquad \overline{R_{n,m}R_{j,k}^*} = \delta_{n,j}\delta_{m,k}. \tag{170}$$

The way to think about this is as follows: if we consider $E_{n,m}$ to lie inside some small, fixed energy shell, then apart from the diagonal matrix elements $\mathcal{O}_{m,n}$ looks like a *random matrix*. This is because in this situation $S(\bar{E}$ and $f_\mathcal{O}(\bar{E},\omega)$ are approximately constant. ETH is a statistical statement in the sense that *typical* matrix elements are believed to obey it.

10.1   ETH and thermalization

We have used the ETH above to compute long-time averages

$$\overline{O} \equiv \lim_{T\to\infty} \frac{1}{T} \int_0^T dt \ \langle \psi(t)|\mathcal{O}|\psi(t)\rangle \ , \tag{171}$$

and show that they agree with results of the micro-canonical ensemble (up to finite-size corrections). We now go a bit further and use it to calculate the time-average of fluctuations of expectation values

$$\sigma_\mathcal{O}^2 \equiv \lim_{T\to\infty} \frac{1}{T} \int_0^T dt \ \big[\langle \psi(t)|\mathcal{O}|\psi(t)\rangle - \overline{\mathcal{O}}\big]^2 . \tag{172}$$

By writing $|\psi(t)\rangle = \sum_n C_n e^{-iE_n t}|n\rangle$ as a linear combination of energy eigenstates we have

$$\sigma_\mathcal{O}^2 = \lim_{T\to\infty} \frac{1}{T} \int_0^T dt \left[\sum_{n,m,p,q} e^{-it(E_n - E_m + E_q - E_p)}\langle m|\mathcal{O}|n\rangle \ \langle p|\mathcal{O}|q\rangle \ C_n C_m^* C_q C_p^* - \overline{\mathcal{O}}^2 \right]$$

$$= \lim_{T\to\infty} \frac{1}{T} \int_0^T dt \sum_{n\neq m, p\neq q} e^{-it(E_n - E_m + E_q - E_p)}\langle m|\mathcal{O}|n\rangle \ \langle p|\mathcal{O}|q\rangle \ C_n C_m^* C_q C_p^*. \tag{173}$$

We now make use that the expansion coefficients $C_n = \langle n|\psi(0)\rangle$ are strongly peaked in energy (see the discussion in subsection 9.1) and the ETH to conclude that the RHS is exponentially small in system size. This means that for large systems the expectation value is most of the time extremely close to its infinite time average, i.e. temporal fluctuations of the expectation value are very small.

Part IV
BBGKY AND QBE

11   BBGKY Hierarchy

We now turn to methods for analyzing non-equilibrium dynamics in *interacting* many-particle systems. For the sake of definiteness let us consider a model of interacting spinless fermions

$$H = -J\sum_{j=1}^{L}(c_j^\dagger c_{j+1} + c_{j+1}^\dagger c_j) - \mu\sum_j n_j + \sum_j \sum_m U_m n_j n_{j+m} \ , \tag{174}$$

where we define $U_{m<1} = 0$. This model has a $U(1)$ symmetry corresponding to particle number conservation

$$U^\dagger c_j U = e^{i\varphi}c_j \ , \tag{175}$$

which simplifies the following discussion. It is convenient to work in momentum space, where the Hamiltonian reads

$$H = \sum_k \epsilon(k)c^\dagger(k)c(k) + \frac{1}{L}\sum_{\boldsymbol{k}} V(k_1,k_2,k_3,k_4)c_{k_1}^\dagger c_{k_2}^\dagger c_{k_3}c_{k_4} \ , \tag{176}$$

where (using that V can be taken to be antisymmetric in $k_{1,2}$ and in $k_{3,4}$ due to the anticommutation relations of the c's)

$$V(\boldsymbol{k}) = \frac{1}{4} \delta_{k_1+k_2, k_3+k_4} \sum_{\ell \geq 1} U_\ell \left[e^{i\ell(k_2-k_3)} - e^{i\ell(k_2-k_4)} - e^{i\ell(k_1-k_3)} + e^{i\ell(k_1-k_4)} \right]. \tag{177}$$

Let $\rho(0)$ be an U(1)-invariant initial density matrix

$$U\rho(0)U^\dagger = \rho(0). \tag{178}$$

11.1 First quantized form of the Hamiltonian

A general n-particle state can be written as

$$|\Psi\rangle = \sum_{j_1 < \cdots < j_n} \Psi(\boldsymbol{j}) c_{j_1}^\dagger \ldots c_{j_n}^\dagger |0\rangle , \tag{179}$$

where $\Psi(\boldsymbol{j})$ is the n-particle wave-function. The position representation of the Hamiltonian is then

$$\begin{aligned}
\mathcal{H}(\boldsymbol{j}, \boldsymbol{k}) &= \langle 0 | c_{j_n} \ldots c_{j_1} H c_{k_1}^\dagger \ldots c_{k_n}^\dagger | 0 \rangle \\
&= \sum_{s=1}^{n} [-J\delta_{k_s, j_s+1} - J\delta_{k_s, j_s-1} - \mu\delta_{k_s, j_s}] \prod_{r \neq s} \delta_{k_r, j_r} + \prod_r \delta_{k_r, j_r} \sum_{w>s} \sum_{m \geq 1} U_m \, \delta_{j_s+m, j_w}.
\end{aligned} \tag{180}$$

11.2 Equations of motion for n-particle Green's functions

Then the probability distributions of all observables can be extracted from the n-particle Geeen's functions

$$G^{(n)}(\boldsymbol{j}; \boldsymbol{\ell}, t) = \text{Tr}\left[\rho(t) c_{j_1}^\dagger \ldots c_{j_n}^\dagger c_{\ell_n} \ldots c_{\ell_1} \right] , \; j_1 < j_2 < \cdots < j_n , \; \ell_1 < \ell_2 < \cdots < \ell_n. \tag{181}$$

The equations of motion for the GFs are

$$\begin{aligned}
i\frac{\partial}{\partial t} G^{(n)}(\boldsymbol{j}; \boldsymbol{\ell}, t) &= \text{Tr}\left[i\dot{\rho}(t) c_{j_1}^\dagger \ldots c_{j_n}^\dagger c_{\ell_n} \ldots c_{\ell_1} \right] = \text{Tr}\left[[H, \rho(t)] c_{j_1}^\dagger \ldots c_{j_n}^\dagger c_{\ell_n} \ldots c_{\ell_1} \right] \\
&= \text{Tr}\left(\rho(t) [c_{j_1}^\dagger \ldots c_{j_n}^\dagger c_{\ell_n} \ldots c_{\ell_1}, H] \right).
\end{aligned} \tag{182}$$

We have

$$[c_{j_1}^\dagger \ldots c_{j_n}^\dagger c_{\ell_n} \ldots c_{\ell_1}, H] = c_{j_1}^\dagger \ldots c_{\ell_2} [c_{\ell_1}, H] + c_{j_1}^\dagger \ldots c_{\ell_3} [c_{\ell_2}, H] c_{\ell, 1} + \cdots + [c_{j_1}^\dagger, H] c_{j_2}^\dagger \ldots c_{\ell_1}, \tag{183}$$

where the basic commutators are given by

$$[c_\ell, H] = \sum_{r=1}^{L} [-J\delta_{\ell+1, r} - J\delta_{\ell-1, r} - \mu\delta_{\ell, r}] c_r + \sum_{s=1}^{L} (U_{s-\ell} + U_{\ell-s}) n_s c_\ell ,$$

$$[c_j^\dagger, H] = \sum_{r=1}^{L} [J\delta_{j+1, r} - J\delta_{j-1, r} - \mu\delta_{j, r}] c_r - \sum_{s=1}^{L} (U_{s-j} + U_{j-s}+) c_j^\dagger n_s. \tag{184}$$

Let us focus on the contribution from $c_{j_1}^\dagger \ldots c_{\ell_2} [c_{\ell_1}, H]$: this can be written as

$$\begin{aligned}
\sum_{r=1}^{L} [-J\delta_{\ell_1+1, r} - J\delta_{\ell_1-1, r} - \mu\delta_{\ell_1, r}] c_{j_1}^\dagger \ldots c_{\ell_2} c_r + \sum_{r=1}^{L} (U_{r-\ell_1} + U_{\ell_1-r}) c_{j_1}^\dagger \ldots c_{j_n}^\dagger c_r^\dagger c_r c_{\ell_n} \ldots c_{\ell_1} \\
+ \sum_{s=2}^{n} U_{\ell_s - \ell_1} c_{j_1}^\dagger \ldots c_{\ell_1} ,
\end{aligned} \tag{185}$$

where the last term arises from moving the $c_r^\dagger c_r$ to the left of c_{ℓ_n}. Putting everything together we arrive at the following hierarchy of equations of motion

$$
\begin{aligned}
i\frac{\partial}{\partial t}G^{(n)}(\boldsymbol{j};\boldsymbol{\ell},t) = & \sum_{\boldsymbol{\ell'}}\mathcal{H}(\boldsymbol{\ell},\boldsymbol{\ell'})G^{(n)}(\boldsymbol{j};\boldsymbol{\ell'},t) - \sum_{\boldsymbol{j'}}\mathcal{H}(\boldsymbol{j},\boldsymbol{j'})G^{(n)}(\boldsymbol{j'};\boldsymbol{\ell},t) \\
& + \sum_{m=1}^{n}\sum_{s=1}^{L}\left[U_{s-\ell_m} + U_{\ell_m - s} - U_{s-j_m} - U_{j_m - s}\right]G^{(n+1)}(\boldsymbol{j},s;s,\boldsymbol{\ell},t)\;.
\end{aligned}
\tag{186}
$$

This is known as the **Bogoliubov-Born-Green-Kirkwood-Yvon hierarchy**. We see that as a result of interactions the equation of motion for the single-particle Green's function involves the two-particle Green's function, the equation of motion for the two-particle Green's function involves the three-particle Green's function and so on.

If our density matrix $\rho(0)$ describes a state with at most N particles, the hierarchy truncates because $G^{(m>N)}(\boldsymbol{j};\boldsymbol{k},t) = 0$. However, for a many-particle system the hierarchy is much too difficult to solve numerically and has to be truncated in some way.

11.3   BBGKY in momentum space

The Green's function in momentum space is

$$
\begin{aligned}
g^{(n)}(\boldsymbol{p};\boldsymbol{q},t) &\equiv \frac{1}{L^n}\sum_{\boldsymbol{j},\boldsymbol{\ell}}e^{-i\boldsymbol{p}\cdot\boldsymbol{j}+i\boldsymbol{q}\cdot\boldsymbol{\ell}}G^{(n)}(\boldsymbol{j};\boldsymbol{\ell},t) \\
&= \mathrm{Tr}\left[\rho(t)c^\dagger(p_1)\ldots c^\dagger(p_n)c(q_n)\ldots c(q_1)\right].
\end{aligned}
\tag{187}
$$

Then the equation of motion for one-particle Green's function in momentum space is

$$
i\frac{\partial}{\partial t}g^{(1)}(p,q,t) = \mathrm{Tr}\left[\rho(t)[c^\dagger(p)c(q),H]\right],
\tag{188}
$$

similar to the previous section. Recall that $H = \sum_k \epsilon(k)c^\dagger(k)c(k) + \frac{1}{L}\sum_{\boldsymbol{k}}V(\boldsymbol{k})c^\dagger(k_1)c^\dagger(k_2)c(k_3)c(k_4)$, where $V(\boldsymbol{k})$ is antisymmetric with respect to exchanging $k_1 \leftrightarrow k_2$ and $k_3 \leftrightarrow k_4$. We have

$$
\begin{aligned}
[c^\dagger(p)c(q),H] = [\epsilon(q) - \epsilon(p)]c^\dagger(p)c(q) + \frac{1}{L}\sum_{\boldsymbol{k}}\Big[& 2V(\boldsymbol{k})c^\dagger(p)c^\dagger(k_2)c(k_3)c(k_4)\delta_{k_1,q} \\
& - 2V(\boldsymbol{k})c^\dagger(k_1)c^\dagger(k_2)c(k_3)c(q)\delta_{k_4,p}\Big].
\end{aligned}
\tag{189}
$$

Therefore, the equation of motion can be written as

$$
i\frac{\partial}{\partial t}g^{(1)}(p,q,t) = [\epsilon(q) - \epsilon(p)]g^{(1)}(p,q,t) + \frac{1}{L}\sum_{\boldsymbol{k},\boldsymbol{k'}}K_1(p,q|k_1,k_2;k_1',k_2')g^{(2)}(\boldsymbol{k};\boldsymbol{k'},t),
\tag{190}
$$

where the integration kernel is defined as

$$
K_1(p,q|k_1,k_2;k_1',k_2') \equiv -2\delta_{k_1,p}V(q,k_2,k_1',k_2') + 2\delta_{k_2',q}V(k_1,k_2,k_1',p).
\tag{191}
$$

Similarly, one can derive the BBGKY hierarchy in momentum space. We summarize the first two as follows:

$$
\begin{aligned}
i\frac{\partial}{\partial t}g^{(1)}(p;q,t) = & \left[\epsilon(q) - \epsilon(p)\right]g^{(1)}(p;q,t) \\
& + \frac{1}{L}\sum_{\boldsymbol{k}_2,\boldsymbol{k}_2'}K_1(p,q|\boldsymbol{k}_2;\boldsymbol{k}_2')g^{(2)}(\boldsymbol{k}_2;\boldsymbol{k}_2',t),
\end{aligned}
\tag{192}
$$

$$i\frac{\partial}{\partial t}g^{(2)}(\boldsymbol{p};\boldsymbol{q},t) = \left[\epsilon(q_1) + \epsilon(q_2) - \epsilon(p_1) - \epsilon(p_2)\right]g^{(2)}(\boldsymbol{p};\boldsymbol{q},t)$$
$$+ \sum_{\boldsymbol{k}_2,\boldsymbol{k}_2'} K_2(\boldsymbol{p},\boldsymbol{q}|\boldsymbol{k}_2;\boldsymbol{k}_2')g^{(2)}(\boldsymbol{k}_2;\boldsymbol{k}_2',t) \tag{193}$$
$$+ \sum_{\boldsymbol{k}_3,\boldsymbol{k}_3'} K_3(\boldsymbol{p},\boldsymbol{q}|\boldsymbol{k}_3;\boldsymbol{k}_3')g^{(3)}(\boldsymbol{k}_3;\boldsymbol{k}_3',t).$$

The kernels $K_{1,2,3}$ are linear in $V(\boldsymbol{k})$.

12   Self-consistent time-dependent mean-field approximation

Truncating the hierarchy: For a meaningful approximation, we need to truncate the hierarchy, which calls for a small parameter. To this end, we assume that $V(k)$ is small, and that we are working in the weakly interacting limit.

In absence of any interactions, the equations of motion are

$$i\frac{\partial}{\partial t}g^{(n)}(\boldsymbol{p};\boldsymbol{q},t) = \underbrace{\left[\sum_{s=1}^{n}\epsilon(q_s) - \epsilon(p_s)\right]}_{E(\boldsymbol{p},\boldsymbol{q})}g^{(n)}(\boldsymbol{p};\boldsymbol{q},t), \tag{194}$$

and the solutions are

$$g^{(n)}(\boldsymbol{p};\boldsymbol{q},t) = e^{-iE(\boldsymbol{p},\boldsymbol{q})t}g^{(n)}(\boldsymbol{p};\boldsymbol{q},0). \tag{195}$$

Therefore, if we further assume that the initial state $\rho(0)$ is a Gaussian fermionic state, which inherently obeys Wick's theorem, we have the following relations at all times:

$$g^{(2)}(\boldsymbol{p};\boldsymbol{q},t) = g^{(1)}(p_1,q_1,t)g^{(1)}(p_2,q_2,t) - g^{(1)}(p_1,q_2,t)g^{(1)}(p_2,q_1,t), \tag{196}$$

$$g^{(3)}(\boldsymbol{p};\boldsymbol{q},t) = \prod_{j=1}^{3}g^{(1)}(p_j,q_j,t) + [\text{all other contractions}]. \tag{197}$$

Physically, this suggests that all connected higher-point correlations functions vanish. One way of truncating the BBGKY hierarchy in the weakly interacting limit is then to assume that the connected higher-point correlations remain small. If we assume that the connected 4-point correlation functions are negligible, i.e.,

$$g^{(2)}(\boldsymbol{p};\boldsymbol{q},t) \approx g^{(1)}(p_1,q_1,t)g^{(1)}(p_2,q_2,t) - g^{(1)}(p_1,q_2,t)g^{(1)}(p_2,q_1,t) \quad \text{(with weak interactions)}, \tag{198}$$

we arrive at a **closed**, **nonlinear** evolution equation for $g^{(1)}$:

$$i\frac{\partial}{\partial t}g^{(1)}(p,q,t) = \left[\epsilon(q) - \epsilon(p)\right]g^{(1)}(p,q,t)$$
$$+ \frac{1}{L}\sum_{\boldsymbol{k},\boldsymbol{k}'}K_1(p,q|\boldsymbol{k};\boldsymbol{k}')\left[g^{(1)}(k_1,k_1',t)g^{(1)}(k_2,k_2',t) - g^{(1)}(k_1,k_2',t)g^{(1)}(k_2,k_1',t)\right]. \tag{199}$$

This corresponds to a time-dependent self-consistent mean-field approximation, i.e., treating the interaction terms in a time-dependent way in the mean-field approximation. Schematically,

$$c_1^\dagger c_2^\dagger c_3 c_4 \rightarrow \begin{array}{ll} c_1^\dagger c_4 \overbrace{\left\langle c_2^\dagger c_3 \right\rangle_t}^{\text{Tr}[\rho(t)c_2^\dagger c_3]} & + \left\langle c_1^\dagger c_4 \right\rangle_t c_2^\dagger c_3 \\ -c_1^\dagger c_3 \left\langle c_2^\dagger c_4 \right\rangle_t & - \left\langle c_1^\dagger c_3 \right\rangle_t c_2^\dagger c_4 \\ - \left\langle c_1^\dagger c_4 \right\rangle_t \left\langle c_2^\dagger c_3 \right\rangle_t & + \left\langle c_1^\dagger c_3 \right\rangle_t \left\langle c_2^\dagger c_4 \right\rangle_t . \end{array} \tag{200}$$

Under this replacement, we have a time-dependent mean-field Hamiltonian

$$\boxed{H_{\text{MF}}(t) = \sum_k \epsilon(k) n(k) + \frac{1}{L} \sum_{p,q} V_{\text{MF}}(p,q,t) c^\dagger(p) c(q) + \varphi(t),} \tag{201}$$

where

$$V_{\text{MF}}(p,q,t) = \sum_{k,k'} 4V(p,k,k',q) \left\langle c^\dagger(k)c(k') \right\rangle_t, \quad \text{by antisymmetry of } V(\boldsymbol{k}), \tag{202}$$

and

$$\varphi(t) = \frac{1}{L} \sum_{\boldsymbol{k}} 2V(\boldsymbol{k}) \left\langle c^\dagger(k_1)c(k_3) \right\rangle_t \left\langle c^\dagger(k_2)c(k_4) \right\rangle_t. \tag{203}$$

Operators in the Heisenberg picture can be written as

$$O_H(t) = U^\dagger(t) O_H(0) U(t). \tag{204}$$

Thus,

$$\begin{aligned} \dot{O}_H(t) &= \dot{U}^\dagger(t) O_H(0) U(t) + U^\dagger(t) O_H(0) \dot{U}(t) \\ &= \left(\dot{U}^\dagger(t) U(t) \right) O_H(t) + O_H(t) \left(U^\dagger(t) \dot{U}(t) \right) \\ &= i[H_H(t), O_H(t)], \end{aligned} \tag{205}$$

where in the last equality, we have used $\dot{U} = -iH(t)U \Rightarrow \dot{U}U^\dagger = -iH(t)$, so $U^\dagger \dot{U} = -iU^\dagger(t)H(t)U(t) = -iH_H(t)$. Also, since $\frac{d}{dt}\left(U^\dagger U \right) = \dot{U}^\dagger U + U^\dagger \dot{U} = 0$, we have $\dot{U}^\dagger U = -U^\dagger \dot{U}$. Here, the unitary operator $U(t)$ can be represented through the time-ordered exponential

$$\begin{aligned} U(t) &= \mathcal{T} e^{-i \int_0^t dt' H(t')} \\ &= 1 - i \int_0^t dt' H(t') - \int_0^t dt' \int_0^{t'} dt'' H(t') H(t'') + \dots \end{aligned} \tag{206}$$

Finally, the equation of motion can be written as

$$\dot{O}_H(t) = iU^\dagger(t)[H(t), O_H(0)]U(t). \tag{207}$$

Thus when applied to the fermionic operators, we have

$$\begin{aligned} \dot{c}(q,t) &= iU^\dagger(t)[H_{\text{MF}}(t), c(q)]U(t) \\ &= iU^\dagger(t) \left[-\epsilon(q)c(q) - \frac{1}{L} \sum_k V_{\text{MF}}(q,k,t)c(k) \right] U(t) \\ &= -i\epsilon(q)c(q,t) - \frac{i}{L} \sum_k V_{\text{MF}}(q,k,t)c(k,t). \end{aligned} \tag{208}$$

Hence,

$$\left.\frac{\partial}{\partial t}g^{(1)}(p,q,t)\right|_{\mathrm{MF}} = \mathrm{Tr}\left[\rho(0)\left(\dot{c}^{\dagger}(p)c(q)+c^{\dagger}(p)\dot{c}(q)\right)\right]$$

$$= i\left[\epsilon(p)-\epsilon(q)\right]g^{(1)}(p,q,t)+\frac{i}{L}\sum_{k}\left[V_{\mathrm{MF}}(k,p,t)g^{(1)}(k,q,t)-V_{\mathrm{MF}}(q,k,t)g^{(1)}(p,k,t)\right]. \tag{209}$$

By recalling

$$V_{\mathrm{MF}}(p,q,t)=\sum_{k,k'}4V(p,k,k',q)g^{(1)}(k,k',t), \tag{210}$$

we arrive at the equivalent closed, nonlinear evolution equation for the 2-point correlation functions shown previously, effectively truncating the BBGKY hierarchy.

13 Quantum Boltzmann equation

Starting from the first two levels of BBGKY in momentum space,

$$i\frac{\partial}{\partial t}g^{(1)}(p;q,t) = \left[\epsilon(q)-\epsilon(p)\right]g^{(1)}(p;q,t)$$
$$+\frac{1}{L}\sum_{\boldsymbol{k}_2,\boldsymbol{k}_2'}K_1(p,q|\boldsymbol{k}_2;\boldsymbol{k}_2')g^{(2)}(\boldsymbol{k}_2;\boldsymbol{k}_2',t), \tag{211}$$

$$i\frac{\partial}{\partial t}g^{(2)}(\boldsymbol{p};\boldsymbol{q},t) = E(\boldsymbol{p},\boldsymbol{q})g^{(2)}(\boldsymbol{p};\boldsymbol{q},t)$$
$$+\sum_{\boldsymbol{k}_2,\boldsymbol{k}_2'}K_2(\boldsymbol{p},\boldsymbol{q}|\boldsymbol{k}_2;\boldsymbol{k}_2')g^{(2)}(\boldsymbol{k}_2;\boldsymbol{k}_2',t)$$
$$+\sum_{\boldsymbol{k}_3,\boldsymbol{k}_3'}K_3(\boldsymbol{p},\boldsymbol{q}|\boldsymbol{k}_3;\boldsymbol{k}_3')g^{(3)}(\boldsymbol{k}_3;\boldsymbol{k}_3',t), \tag{212}$$

we take the following steps:

Step 1: Integrate the 2nd equation over time.
First notice that the second equation can be rewritten as

$$i\partial_t\left(e^{iEt}g^{(2)}\right) = e^{iEt}\left[i\partial_t g^{(2)}-Eg^{(2)}\right] = e^{iEt}\left[\sum K_2g^{(2)}+\sum K_3g^{(3)}\right]. \tag{213}$$

Integrating this equation over time, we have

$$g^{(2)}(\boldsymbol{p};\boldsymbol{q},t) = e^{-iE(\boldsymbol{p},\boldsymbol{q})t}g^{(2)}(\boldsymbol{p};\boldsymbol{q},0)$$
$$-i\int_0^t \mathrm{d}t' e^{-iE(\boldsymbol{p},\boldsymbol{q})(t-t')}\sum_{\boldsymbol{k}_2,\boldsymbol{k}_2'}K_2(\boldsymbol{p},\boldsymbol{q}|\boldsymbol{k}_2;\boldsymbol{k}_2')g^{(2)}(\boldsymbol{k}_2;\boldsymbol{k}_2',t)$$
$$-i\int_0^t \mathrm{d}t' e^{-iE(\boldsymbol{p},\boldsymbol{q})(t-t')}\sum_{\boldsymbol{k}_3,\boldsymbol{k}_3'}K_3(\boldsymbol{p},\boldsymbol{q}|\boldsymbol{k}_3;\boldsymbol{k}_3')g^{(3)}(\boldsymbol{k}_3;\boldsymbol{k}_3',t), \tag{214}$$

Step 2: Assume that the higher-point connected correlators are negligible, so

$$g^{(2)}(\boldsymbol{k}_2;\boldsymbol{k}_2',t) \approx \mathcal{A}_{[k_1,k_2]}g^{(1)}(k_1,k_1',t)g^{(1)}(k_2,k_2',t), \tag{215}$$

$$g^{(3)}(\boldsymbol{k}_3; \boldsymbol{k}'_3, t) \approx \mathcal{A}_{[k_1,k_2,k_3]} \prod_{j=1}^{3} g^{(1)}(k_j, k'_j, t), \tag{216}$$

where $\mathcal{A}_{[\cdots]}$ indicates a fully antisymmetric sum over the indices.

Step 3: Substitute into the 1st equation, we have

$$
\begin{aligned}
i\frac{\partial}{\partial t} g^{(1)}(p,q,t) &= [\epsilon(q) - \epsilon(p)] \, g^{(1)}(p,q,t) \\
&+ \frac{1}{L} \sum_{\boldsymbol{k}_2, \boldsymbol{k}'_2} 2K_1(p,q|\boldsymbol{k}_2; \boldsymbol{k}'_2) e^{-iE(\boldsymbol{k}_2, \boldsymbol{k}'_2)t} g^{(1)}(k_1, k'_1, 0) g^{(1)}(k_2, k'_2, 0) \\
&- i \int_0^t dt' \frac{1}{L} \sum_{\boldsymbol{k}_2, \boldsymbol{k}'_2} M_2(p,q|\boldsymbol{k}_2, \boldsymbol{k}'_2, t-t') g^{(1)}(k_1, k'_1, t) g^{(1)}(k_2, k'_2, t) \\
&- i \int_0^t dt' \frac{1}{L} \sum_{\boldsymbol{k}_3, \boldsymbol{k}'_3} M_3(p,q|\boldsymbol{k}_3, \boldsymbol{k}'_3, t-t') \prod_{j=1}^{3} g^{(1)}(k_j, k'_j, t),
\end{aligned}
\tag{217}
$$

where

$$M_n(p,q|\boldsymbol{k}_n, \boldsymbol{k}'_n, t-t') \equiv n! \sum_{\boldsymbol{Q}_2, \boldsymbol{Q}'_2} K_1(p,q|\boldsymbol{Q}_2, \boldsymbol{Q}'_2) K_n(\boldsymbol{Q}_2, \boldsymbol{Q}'_2|\boldsymbol{k}_n, \boldsymbol{k}'_n) e^{-iE(\boldsymbol{Q}_2, \boldsymbol{Q}'_2)(t-t')}. \tag{218}$$

This is the 2nd Born approximation, namely

- The dynamics is non-Markovian, i.e., $g^{(1)}(p,q,t)$ depends on all $g^{(1)}(p,q,t' < t)$.

- K_1 is of order $\mathcal{O}(V)$, and $M_{2,3}$ of order $\mathcal{O}(V^2)$.

If we further restrict our attention to translationally invariant system, we have

$$
\begin{aligned}
g^{(1)}(p,q,t) = \mathrm{Tr}\left[\rho(t) c^\dagger(p) c(q)\right] &= \delta_{p,q} \mathrm{Tr}\left[\rho(t) n(p)\right] \\
&= \delta_{p,q} f(p,t),
\end{aligned}
\tag{219}
$$

where $f(p,t)$ denotes fermion occupation number. And since $V(k_1, k_2, k_3, k_4) \propto \delta_{k_1+k_2, k_3+k_4}$, the 1st-order term $\propto K_1$ now vanishes.

In this situation, the equation of motion simplifies to

$$
\begin{aligned}
\dot{f}(p,t) = &-\int_0^t dt' \frac{1}{L^2} \sum_{\boldsymbol{k}} e^{-i(t-t')[\epsilon(k_1)+\epsilon(k_2)-\epsilon(k_3)-\epsilon(k_4)]} \times 8\,|V(\boldsymbol{k})|^2 \times [\delta_{k_4,p} - \delta_{k_1,p}] \\
&\times \left[f(k_1,t) f(k_2,t) \bar{f}(k_3,t) \bar{f}(k_4,t) - f(k_3,t) f(k_4,t) \bar{f}(k_1,t) \bar{f}(k_2,t)\right]
\end{aligned}
\tag{220}
$$

where we have exploited $V(k_1, k_2, k_3, k_4) = V^*(k_3, k_4, k_1, k_2)$ and defined $\bar{f}(k,t) \equiv 1 - f(k,t)$. Note that the quartic terms in f cancel (as required). This is now an evolution equation for the fermionic mode occupation.

Step 4: Local approximation in time

It is convenient to introduce an explicit small parameter

$$V(\boldsymbol{k}) = \lambda \bar{V}(\boldsymbol{k}), \tag{221}$$

and use the relation

$$e^{-iE_0(t-t')} = \int_{-\infty}^{\infty} \mathrm{d}E \delta(E - E_0) e^{-iE(t-t')} \tag{222}$$

to rewrite the equation as

$$-\frac{\partial}{\partial t} f(p, t) = \lambda^2 \int_{-\infty}^{\infty} \mathrm{d}E \int_0^t \mathrm{d}t' e^{-iE(t-t')} \gamma(E, p, t'), \tag{223}$$

where the integrand is summarised in $\gamma(E, p, t')$. Now, consider a rescaled time $\tau \equiv \lambda^2 t$, so $\frac{1}{\lambda^2}\frac{\partial}{\partial t} = \frac{\partial}{\partial \tau}$. We may write the equation in this new time scale as

$$
\begin{aligned}
-\frac{\partial}{\partial \tau} f\left(p, \frac{\tau}{\lambda^2}\right) &= \int_{-\infty}^{\infty} \mathrm{d}E \int_0^\tau \frac{\mathrm{d}s}{\lambda^2} e^{-iE\frac{\tau-s}{\lambda^2}} \gamma\left(E, p, \frac{s}{\lambda^2}\right) \\
&= \int_0^\tau \frac{\mathrm{d}s}{\lambda^2} \tilde{\gamma}\left(\frac{\tau-s}{\lambda^2}, p, \frac{s}{\lambda^2}\right),
\end{aligned} \tag{224}
$$

where $\tilde{\gamma}$ is the Fourier transform of γ in the E argument. Under another change of variable, $u = \frac{\tau-s}{\lambda^2}$, we arrive at

$$-\frac{\partial}{\partial \tau} f\left(p, \frac{\tau}{\lambda^2}\right) = \int_0^{\tau/\lambda^2} \mathrm{d}u \tilde{\gamma}\left(u, p, \frac{\tau - u\lambda^2}{\lambda^2}\right). \tag{225}$$

In the weakly interacting limit, we shall assume that the following limits exist:

$$\lim_{\lambda \to 0} f(p, \tau/\lambda^2) = F(p, \tau), \tag{226}$$

$$\lim_{\lambda \to 0} \gamma(E, p, \tau/\lambda^2) = \Gamma(E, p, \tau), \tag{227}$$

namely that there exists a universal dynamical behavior in the rescaled time. Then, assuming that the integral and the weak interaction limit commutes,

$$
\begin{aligned}
-\frac{\partial}{\partial \tau} F(p, \tau) &= \lim_{\lambda \to 0} \int_0^{\tau/\lambda^2} \mathrm{d}u \tilde{\Gamma}(u, p, \tau - \lambda^2 u) \\
&= \int_0^\infty \mathrm{d}u \tilde{\Gamma}(u, p, \tau) = \frac{1}{2} \int_{-\infty}^\infty \mathrm{d}u \tilde{\Gamma}(u, p, \tau) \\
&= \pi \Gamma(0, p, \tau).
\end{aligned} \tag{228}
$$

This gives

$$
\boxed{
\begin{aligned}
-\frac{\partial}{\partial \tau} F(p, \tau) = \frac{1}{L^2} \sum_{\boldsymbol{k}} 8\pi \left|V(\boldsymbol{k})\right|^2 \left[\delta_{k_4,p} - \delta_{k_1,p}\right] \delta\left(\epsilon(k_1) + \epsilon(k_2) - \epsilon(k_3) - \epsilon(k_4)\right) \\
\times \left[F(k_1, \tau)F(k_2, \tau)\bar{F}(k_3, \tau)\bar{F}(k_4, \tau) - F(k_3, \tau)F(k_4, \tau)\bar{F}(k_1, \tau)\bar{F}(k_2, \tau)\right],
\end{aligned}
} \tag{229}
$$

and this is known as the quantum Boltzmann equation (QBE). The QBE is a standard approach in many-particle dynamics. Some comments are in order:

- The QBE, strictly speaking, applies in the Boltzmann scaling limit, in which $\lambda \to 0$ and $t \to \infty$ while $\lambda^2 t = \tau$ is fixed.

- The QBE is a Markovian evolution equation.

- Generically, this is only applicable at sufficiently late times; for short times one should use the non-Markovian 2nd Born approximation derived in Step 3.

- Instead of weak interactions ($\lambda \to 0$), one can also use the low-density limit to formulate a QBE.

- One can also consider non-translationally invariant situations, though the derivations are more complicated and equations would be modified.

Part V
QUANTUM MASTER EQUATIONS

Consider a QM many-particle system interacting with an "environment":

- Hilbert space: $\mathcal{H} = \mathcal{H}_S \otimes \mathcal{H}_E$. We denote the respective dimensions by $D_{S,E}$.

- The Hamiltonian can be written in the form

$$H = H_S + H_E + H_{\text{int}}. \tag{230}$$

  where H_S and H_E only act on the system and environment degrees of freedom respectively.

- We will assume that there are no initial correlations between the system and the bath degrees of freedom. This is implies that the initial density matrix is

$$\rho(0) = \rho_S(0) \otimes \rho_E(0). \tag{231}$$

The time evolution of system plus environment is given by the time-dependent Schrödinger equation

$$\rho(t) = U(t)\rho(0)U^{\dagger}(t) , \qquad U(t) = e^{-iHt} . \tag{232}$$

From a physics point of view we are not interested in the environment but only the system itself. The reduced density matrix describing the time evolution of the system degrees of freedom is

$$\rho_S(t) = \text{Tr}_E\left[\rho(t)\right] = \text{Tr}_E\left[U(t)\rho(0)U^{\dagger}(t)\right]. \tag{233}$$

It is useful to think of this in terms of a *completely positive, trace-preserving map* $\mathcal{M}_t$

$$\rho_S(t) = \mathcal{M}_t[\rho_S(0)]. \tag{234}$$

By construction the map $\mathcal{M}_t$ has the following properties

(M1) $\mathcal{M}_t$ is trace preserving.

Initially we have by construction

$$\text{Tr}_S[\rho_S(0)] = \text{Tr}[\rho_S(0) \otimes \rho_E(0)] = 1. \tag{235}$$

At later times we have

$$\begin{aligned}
\text{Tr}_S[\rho_S(t)] &= \text{Tr}_S\big[\text{Tr}_E\big[U(t)\big(\rho_S(0) \otimes \rho_E(0)\big)U^{\dagger}(t)\big] = \text{Tr}\big[U(t)\big(\rho_S(0) \otimes \rho_E(0)\big)U^{\dagger}(t)\big] \\
&= \text{Tr}\big[\rho_S(0) \otimes \rho_E(0)\big] = 1.
\end{aligned} \tag{236}$$

(M2) $\mathcal{M}_t$ preserves Hermiticity of the reduced density matrix.

$$\rho_S(0) = \left(\rho_S(0)\right)^\dagger \Rightarrow \rho_S(t) = \left(\rho_S(t)\right)^\dagger . \tag{237}$$

(M3) $\mathcal{M}_t$ is *positive*, meaning that

$$\text{eigenvalues of } \rho_S(0) \geq 0 \Rightarrow \text{eigenvalues of } \rho_S(t) \geq 0. \tag{238}$$

(M4) $\mathcal{M}_t$ is *completely positive*, meaning that for any k

$$\text{Id}_{k \times k} \otimes \mathcal{M}_t \text{ is positive over } \text{End}\left(\mathbb{C}^k \otimes \mathcal{H}_S\right). \tag{239}$$

To see this, consider a positive operator B on $\mathbb{C}^k \otimes \mathcal{H}_S$ and write our map $\mathcal{M}_t$ in an orthonormal basis $\{|k\rangle\}$ of $\mathcal{H}_E$

$$(\text{Id} \otimes \mathcal{M}_t)[B] = \text{Id} \otimes \sum_k \langle k|UBU^\dagger|k\rangle . \tag{240}$$

This is a sum of positive operators and hence positive.

> **Aside 2:**
>
> Complete positivity is a stronger property than positivity: not every positive map is completely positive. An example is *transposition*
>
> $$\mathcal{M}[\rho] = \rho^T . \tag{241}$$
>
> $\mathcal{M}$ is clearly positive as it does not change the eigenvalues of ρ. To be specific take $\mathcal{H}_S = \mathbb{C}^2$ and $k = 2$. Defining a basis of 2×2 matrices by
>
> $$\left(e^{ab}\right)_{ij} = \delta_{a,i}\delta_{b,j} , \tag{242}$$
>
> we consider the particular operator
>
> $$X = \begin{pmatrix} e^{11} & e^{12} \\ e^{21} & e^{22} \end{pmatrix} \in \text{End}\left(\mathbb{C}^2 \otimes \mathcal{H}_S\right). \tag{243}$$
>
> The eigenvalues of X are $\{2, 0, 0, 0\}$. The transposition map acts as
>
> $$\left[\text{Id}_{2 \times 2} \otimes \mathcal{M}\right](X) = \begin{pmatrix} e^{11} & e^{21} \\ e^{12} & e^{22} \end{pmatrix} . \tag{244}$$
>
> This is a permutation operator and has eigenvalues $\{1, 1, 1, -1\}$, i.e. is no longer positive.

We have seen that the time evolution of the reduced density matrix is given by a *completely positive, trace-preserving map* (CPTPM). Conversely, we have

> **Theorem 1:** STINESPRING'S THEOREM
>
> Any CPTPM can be expressed in the form
>
> $$\mathcal{M}[\rho] = \text{Tr}_E\left[U(\rho \otimes \rho_E)U^\dagger\right] \tag{245}$$
>
> for some (non-unique) unitary operator U and density matrix ρ_E.

14 Kraus representation

Let us assume for simplicity that $\rho_E = |0\rangle\langle 0|$ for some $|0\rangle \in \mathcal{H}_E$ and let $\{|k\rangle; k = 0, \dots D_E - 1\}$ an orthonormal basis of $\mathcal{H}_E$. Then we have for a general CPTPM

$$\rho' = \mathrm{Tr}_E\big[U(\rho \otimes |0\rangle\langle 0|)U^\dagger\big]$$
$$= \sum_{k=0}^{D_E-1} \langle k|U|0\rangle \rho \langle 0|U^\dagger|k\rangle. \tag{246}$$

Writing the unitary as

$$U = \sum_{k,\ell=0}^{D_E-1} |k\rangle\langle\ell|\, \mathcal{U}_{k,\ell}\,, \quad \mathcal{U}_{k,\ell} \in \mathrm{End}(\mathcal{H}_S), \tag{247}$$

we obtain

$$\rho' = \sum_{k=0}^{D_E-1} \mathcal{U}_{k,0}\rho\,\mathcal{U}_{k,0}^\dagger. \tag{248}$$

Defining *Kraus operators*

$$K_k = \mathcal{U}_{k,0}\,, \qquad \sum_{k=0}^{D_E-1} K_k^\dagger K_k = \mathbb{1}\,, \tag{249}$$

we arrive at

$$\rho' = \sum_{k=0}^{D_E-1} K_k\rho K_k^\dagger\,. \tag{250}$$

But as $K_k \in \mathrm{End}(\mathcal{H}_S)$ there are only D_s^2 linear independent Kraus operators $\mathcal{K}_k$. This implies that by making an appropriate choice of these we obtain

---

Theorem 2: KRAUS' THEOREM

Any CPTPM can be written in the form

$$\rho' = \mathcal{M}[\rho] = \sum_{k=0}^{r} \mathcal{K}_k\rho\mathcal{K}_k^\dagger\,, \qquad \sum_{k=0}^{r} \mathcal{K}_k\mathcal{K}^\dagger = \mathbb{1}, \tag{251}$$

where the *Kraus rank* $r \leq D_S^2 - 1$.

It is easy to see that the Kraus representation is not unique. For example the set of operators

$$K_n' = \sum_l U_{n,l}\mathcal{K}_l\,, \qquad UU^\dagger = \mathbb{1} \tag{252}$$

fulfils $\sum_n K_n'(K_n')^\dagger = \mathbb{1}$ and

$$\sum_k \mathcal{K}_k\rho\mathcal{K}_k^\dagger = \sum_k K_k'\rho(K_k')^\dagger. \tag{253}$$

14.1 Infinitesimal generators of Kraus maps and Lindblad equation

Let us now consider an infinitesimal time step

$$\rho(t+\delta t) = \mathcal{M}_{t,\delta t}[\rho(t)]$$
$$= \rho(t) + \delta t\dot{\rho}(t) + \mathcal{O}(\delta t^2). \tag{254}$$

There are two types of Kraus operators that generate terms linear in δt:

$$\mathcal{K}_k = \alpha_k \mathbb{1} + \delta t[M_k - iH_k] + o(\delta t) \ , \quad 0 \le k < k_0 \ , \quad \sum_{k=0}^{k_0} \alpha_k = 1 \ , \quad H_k = H_k^\dagger, L_k = L_k^\dagger \ ,$$

$$\mathcal{K}_m = L_m \sqrt{\delta t} + o(\sqrt{\delta t}) \ , \quad m > k_0. \tag{255}$$

This gives

$$\mathcal{M}_{t,\delta t}[\rho(t)] = \rho(t) + \delta t\Big[\sum_{k<k_0} -i\alpha_k[H_k, \rho(t)] + \alpha_k\{M_k, \rho(t)\} + \sum_{n>k_0} L_n\rho(t)L_n^\dagger \Big] + o(\delta t). \tag{256}$$

We see that all terms involving H_k and M_k can be combined into a single contribution. Hence we can without loss of generality take $k_0 = 1$ and define $H_0 = H$, $M_0 = M$. We then can eliminate the M term by solving

$$\mathbb{1} = \sum_k \mathcal{K}_k \mathcal{K}_k^\dagger = \mathbb{1} + \delta t\Big[2M + \sum_k L_k^\dagger L_k\Big] \Rightarrow M = -\frac{1}{2}\sum_k L_k^\dagger L_k \ . \tag{257}$$

Putting everything together we arrive at the *Lindblad equation*[15, 16]

$$\boxed{\frac{d}{dt}\rho_S(t) = -i[H, \rho_s(t)] + \sum_k L_k\rho_S(t)L_k^\dagger - \frac{1}{2}\{L_k^\dagger L_k, \rho_S(t)\}.}$$

$$\tag{258}$$

Here L_k are called *jump operators*. The Lindblad equation has a very suggestive form:

- The first term on the r.h.s. looks like a time-dependent Schrödinger equation with system Hamiltonian H.

- If we think of H as the system Hamiltonian the second term then must describe the effects of the environment on the system.

- The L_k will a priori depend on the full history of the system and environment for all times $t' < t$.

14.2 Markovian approximation

For general environments the time evolution of the system will be very complicated, as its reduced density matrix at time t will depend on the details of its "history", i.e. its state at all times $t' < t$. In order to get something tangible we have to make some simplifying assumptions on the environment and its coupling to the system of interest. For simplicity let's assume that all local correlation functions in the bath decay exponentially in time

$$\mathrm{Tr}_E\big[A_E(x,t)B_E(x)\rho_E\big] \propto e^{-t/\tau_{AB}} \ , \tag{259}$$

and define a typical time scale τ_E associated with quantum dynamics of the bath degrees of freedom as $\max_{A,B}(\tau_{AB})$. The analogous time scale for the system is denoted by τ_S. We then further assume that

(S1) The back-reaction of the system on the environment is negligible.

(S2) The system dynamics (w/o coupling to the environment) is such that the characteristic relaxation time scale is very large compared to the relaxation time of the environment

$$\tau_S \gg \tau_E \ . \tag{260}$$

Under these conditions we can consider a "stroboscopic" time evolution of the system by considering discrete time steps δt such that

$$\tau_S \gg \delta t \gg \tau_E \ . \tag{261}$$

This stroboscopic time evolution is then essentially *Markovian*, i.e. $\rho_S(t + \delta t)$ depends only on the state of the system at time t and not its prior history. However, we still don't really know what H and the L_k in the Lindblad equation are for a given physical problem. To understand this it is very useful to consider systems that are *weakly coupled* to environments.

15 Redfield equation

Let us start with a system that is weakly coupled to an environment

$$H = \underbrace{H_S + H_E}_{H_0} + \lambda V \ , \quad V = \sum_n S_n \otimes E_n \ . \tag{262}$$

Here S_n and E_n are operators acting only on system and environment degrees of freedom respectively and $|\lambda| \ll 1$ is a small parameter. The time-dependent Schrödinger equation is

$$\frac{d\rho(t)}{dt} = -i[H, \rho(t)] \ . \tag{263}$$

Now we go to the *interaction picture* by defining

$$\rho_I(t) = e^{iH_0 t} \rho(t) e^{-iH_0 t} \ , \quad V_I(t) = e^{iH_0 t} V e^{-iH_0 t} \ . \tag{264}$$

A simple calculation using (263) gives

$$\dot{\rho}_I(t) = -i\lambda[V_I(t), \rho_I(t)]. \tag{265}$$

Integrating over time results in an integral equation

$$\rho_I(t) = \rho_I(0) - i\lambda \int_0^t ds [V_I(s), \rho_I(s)]. \tag{266}$$

We can solve this formally by iteration, using that by assumption λ is small

$$\rho_I(t) = \rho_I(0) - i\lambda \int_0^t ds [V_I(s), \rho_I(0)] - \lambda^2 \int_0^t ds \int_0^s ds' [V_I(s), [V_I(s'), \rho_I(t)] + \mathcal{O}(\lambda^3). \tag{267}$$

Here we have used the fact that in the $\mathcal{O}(\lambda^2)$ term we can replace $\rho_I(0)$ by $\rho_I(t)$ up to the order in λ we are working in. Now we define

$$\rho_{I,S}(t) \equiv \mathrm{Tr}_E\big(\rho_I(t)\big), \tag{268}$$

and make the following assumptions/observations:

(i) The environment is time-independent

$$\rho_I(t) \approx \rho_{I,S}(t) \otimes \rho_E(0) \tag{269}$$

(ii) Without loss of generality we may assume that

$$\mathrm{Tr}_E[\rho_E E_k] = 0 \ . \tag{270}$$

This can always be achieved by an appropriate redefinition of the system Hamiltonian. To see this assume that $\langle E_k \rangle = \mathrm{Tr}_E[\rho_E E_k] \neq 0$. Then

$$H = \underbrace{H_S + \lambda \sum_k \langle E_k \rangle S_k}_{H_S'} + H_E + \lambda \sum_k S_k \otimes (E_k - \langle E_k \rangle) \tag{271}$$

Tracing over the environment, using (i) and (ii) and taking the derivative in time we obtain the *Redfield equation*

$$\boxed{\dot{\rho}_{I,S}(t) = -\lambda^2 \int_0^t ds \ \mathrm{Tr}_E\Big[V_I(t), [V_I(s), \rho_{I,S}(t) \otimes \rho_E]\Big] \ .}$$

$$\tag{272}$$

Finally we evaluate the trace for the form of V given in (262)

$$\dot{\rho}_{I,S}(t) = -\lambda^2 \int_0^t ds \sum_{n,m} J_{n,m}(t-s)[S_n(t), S_m(t-s)\rho_{I,S}(t)] + \text{h.c.} , \tag{273}$$

where the matrix $J(t)$ is given by

$$J_{n,m}(t-t') = \text{Tr}_E\left[E_n(t)E_m(t')\rho_E\right] . \tag{274}$$

The main problem with the Redfield equation is that it does not guarantee positivity and trace preservation of the reduced density matrix. In practice this means that it can be used only for sufficiently short times where such effects may be small because of the smallness of λ.

15.1 From Redfield to Lindblad

It is possible to derive a Lindblad equation starting from the Redfield equation, see [17]. As the derivation is somewhat lengthy we only state the results. A key object is the matrix $g(\omega)$ defined as the matrix square root of the Fourier transform of $J_{k,l}(s)$

$$g(\omega) = \sqrt{\frac{J(\omega)}{2\pi}} , \qquad J_{k,l}(\omega) = \int_{-\infty}^{\infty} ds \ J_{k,l}(s)e^{i\omega s}. \tag{275}$$

In terms of these one defines

$$\Gamma = \lambda^2 \left[\int_{-\infty}^{\infty} dt \|g(t)\|_{2,1}\right]^2 , \qquad \tau = \frac{\int_{-\infty}^{\infty} dt \|tg(t)\|_{2,1}}{\int_{-\infty}^{\infty} dt \|g(t)\|_{2,1}} , \tag{276}$$

where the $L_{2,1}$ matrix norm is defined by

$$\|M\|_{2,1} \equiv \sum_k \sqrt{\sum_l |M_{l,k}|^2}. \tag{277}$$

Then, if $\Gamma\tau \ll 1$ one has (up to small corrections)

$$\dot{\rho}_{I,S}(t) = -i[\Lambda_I(t), \rho_{I,S}(t)] + \sum_k \left[L_{k,I}(t)\rho_{I,S}(t)L_{k,I}^\dagger(t) - \frac{1}{2}\{L_{k,I}^\dagger(t)L_{k,I}(t), \rho_{I,S}(t)\}\right] , \tag{278}$$

where

$$L_{k,I}(t) = \lambda \sum_l \int_{-\infty}^{\infty} ds g_{k,l}(t-s)S_{l,I}(s) ,$$

$$\Lambda_I(t) = \frac{\lambda^2}{2i} \int_{-\infty}^{\infty} ds \int_{-\infty}^{\infty} ds' \sum_{k,l} S_{k,I}(s)S_{l,I}(s') \underbrace{g_{k,n}(s-t)g_{n,l}(t-s')\text{sgn}(s-s')}_{\phi_{k,l}(s-t,s'-t)} . \tag{279}$$

Finally we go back to the Schrödinger picture using

$$\rho_{I,S} = \text{Tr}_E\left[e^{iH_0 t}\rho(t)e^{-iH_0 t}\right] = e^{iH_s t}\text{Tr}_E\left[e^{iH_E t}\rho(t)e^{-iH_E t}\right]e^{-iH_s t}$$

$$= e^{iH_s t}\rho_S(t)e^{-iH_s t} . \tag{280}$$

This gives a Lindblad equation

$$\boxed{\begin{array}{l} \rho_S(t) = -i[H_S + \Lambda, \rho_S(t)] + \sum_k L_k \rho_S(t)L_k^\dagger - \frac{1}{2}\{L_k^\dagger L_k, \rho_S(t)\} , \\[2mm] L_k = \lambda \sum_l \int ds \ g_{k,l}(s) \ S_{l,I}(-s) , \\[2mm] \Lambda = \frac{\lambda^2}{2i} \int dsds' \sum_{k,l} \phi_{k,l}(s, s') \ S_{k,I}(s)S_{l,I}(s') . \end{array}}$$

This derivation is instructive because it shows

- how the jump operators L_k arise from the microscopic system-bath interactions;

- that there is contribution Λ to the "coherent" (i.e. von Neumann) part of the Lindblad equation. This is sometimes referred to as "Lamb shift".

Part VI
Periodically driven systems

References

[1] P. Calabrese and J. Cardy, *Evolution of entanglement entropy in one-dimensional systems*, J. Stat. Mech. (2005) P04010.

[2] P. Calabrese and J. Cardy, *Time Dependence of Correlation Functions Following a Quantum Quench*, Phys. Rev. Lett. **96**, 136801 (2006).

[3] M.A. Cazalilla, *Effect of Suddenly Turning on Interactions in the Luttinger Model*, Phys. Rev. Lett. **97**, 156403 (2006).

[4] A. Iucci and M. A. Cazalilla, *Quantum quench dynamics of the Luttinger model*, Phys. Rev. A **80**, 063619 (2009).

[5] A.S. Buyskikh, M. Fagotti, J. Schachenmayer, F.H.L. Essler, A. J. Daley, *Entanglement growth and correlation spreading with variable-range interactions in spin and fermionic tunnelling models*, Phys. Rev. A 93, 053620 (2016) [http://dx.doi.org/10.1103/PhysRevA.93.053620].

[6] E. H. Lieb and D. W. Robinson, *The finite group velocity of quantum spin systems*, Commun. Math. Phys. **28**, 251 (1972).

[7] R. Sims and B. Nachtergaele, *Lieb-Robinson bounds in quantum many-body physics*, edited by R. Sims and D. Ueltschi, Entropy and the Quantum, Vol. 529 (American Mathematical Society, 2010).

[8] S. Bravyi, M. B. Hastings, and F. Verstraete, *Lieb-Robinson Bounds and the Generation of Correlations and Topological Quantum Order*, Phys. Rev. Lett. **97**, 050401 (2006).

[9] L. Bonnes, F.H.L. Essler and A. Läuchli, *"Light-Cone" Dynamics After Quantum Quenches in Spin Chains*, Phys. Rev. Lett. **113**, 187203 (2014).

[10] M. Cheneau, P. Barmettler, D. Poletti, M. Endres, P. Schauss, T. Fukuhara, C. Gross, I. Bloch, C. Kollath, and S. Kuhr, *Light-cone-like spreading of correlations in a quantum many-body system*, Nature **481**, 484 (2012).

[11] T. Langen, R. Geiger, M. Kuhnert, B. Rauer, and J. Schmiedmayer, *Local emergence of thermal correlations in an isolated quantum many-body system*, Nature Physics **9**, 640 (2013).

[12] J. Cardy, *Thermalization and Revivals after a Quantum Quench in Conformal Field Theory*, Phys. Rev. Lett. **112**, 220401 (2014).

[13] B. Rauer, S. Erne, T. Schweigler, F. Cataldini, M. Tajik, J. Schmiedmayer, *Recurrences in an isolated quantum many-body system*, Science **360**, 307 (2018).

[14] M. Srednicki, *The approach to thermal equilibrium in quantized chaotic systems*, J. Phys. **A32**, 1163 (1999).

[15] G. Lindblad, *On the generators of quantum dynamical semigroups*, Comm. Math. Phys. **48**, 119 (1976).

[16] V. Gorini, A. Kossakowski and E.C. Sudarshan, *Completely positive dynamical semigroups of N-level systems*, J. Math. Phys. **17**, 821 (1976).

[17] F. Nathan and M.S. Rudner, *Universal Lindblad equation for open quantum systems*, Phys. Rev. B**102**, 115109 (2020).